



UNIVERSIDADE FEDERAL DE PERNAMBUCO

CENTRO DE TECNOLOGIA E GEOCIÊNCIAS

DEPARTAMENTO DE OCEANOGRÁFIA

PROGRAMA DE PÓS-GRADUAÇÃO EM OCEANOGRÁFIA

BRENNO JANUARIO DA SILVA

CARACTERIZAÇÃO DO SISTEMA CARBONATO NO ARQUIPÉLAGO DE  
FERNANDO DE NORONHA

RECIFE

2018

BRENNO JANUARIO DA SILVA

CARACTERIZAÇÃO DO SISTEMA CARBONATO NO ARQUIPÉLAGO DE  
FERNANDO DE NORONHA

Dissertação apresentada ao Programa de Pós-Graduação em Oceanografia do Departamento de Oceanografia da Universidade Federal de Pernambuco, como requisito para obtenção do título de Mestre em Oceanografia.

Área de concentração: Oceanografia Abiótica

Orientador: Prof. Dr. Manuel de Jesus Flores Montes.

Coorientador: Prof. Dr. Felipe Lima Gaspar.

RECIFE

2018

Catalogação na fonte  
Bibliotecária Margareth Malta, CRB-4 / 1198

S586c Silva, Brenno Januario da.  
Caracterização do sistema carbonato no Arquipélago de Fernando de Noronha / Brenno Januario da Silva – 2018.  
49 folhas, il., gráfs., tabs.

Orientador: Prof. Dr. Manuel de Jesus Flores Montes.  
Coorientador: Prof. Dr. Felipe Lima Gaspar.

Dissertação (Mestrado) – Universidade Federal de Pernambuco. CTG.  
Programa de Pós-Graduação em Oceanografia, 2018.  
Inclui Referências e Apêndice.

1. Oceanografia. 2. Efeito ilha. 3. Carbono inorgânico. 4. Processos turbulentos. 5. Picnoclina. I. Montes, Manuel de Jesus Flores. (Orientador). II. Gaspar, Felipe Lima. (Coorientador). III. Título.

UFPE

551.46 CDD (22. ed.)

BCTG/2018-99

BRENNO JANUARIO DA SILVA

CARACTERIZAÇÃO DO SISTEMA CARBONATO NO ARquipéLAGO DE  
FERNANDO DE NORONHA

Dissertação apresentada ao Programa de Pós-Graduação em Oceanografia do Departamento de Oceanografia da Universidade Federal de Pernambuco, como requisito para obtenção do título de Mestre em Oceanografia.

Aprovado em 08 de fevereiro de 2018.

BANCA EXAMINADORA

---

Dr. Felipe Lima Gaspar (Co-orientador) – Presidente, Universidade Federal de Pernambuco

---

Dr. Barbara Ramos Pinheiro – Titular Externo, Universidade Federal de Alagoas

---

Prof. Dr. Marcus André Silva – Titular Interno, Universidade Federal de Pernambuco

O apoio e incansável incentivo aos estudos me trouxeram até aqui. Me tornaram uma pessoa apaixonada pela ciência. Dedico isso inteiramente aos meus pais, Nivaldo Januario e Aurinete

Maria.

## AGRADECIMENTOS

Agradeço primeiramente à minha mãe, Aurinete Maria, e ao meu irmão, Heitor Januario, por me apoiarem de todas as formas possíveis e imagináveis durante minha jornada no mestrado. Faço em nome deles, faço por eles, sem eles jamais conseguiria concluir esta etapa. Ao meu Tio Apiu, Tia Fátima, à minha Madrinha, aos meus primos Poli e Flávio e à minha linda afilhada Malu, obrigado por todo apoio.

Ao meu orientador, Professor Dr. Manuel Flores Montes. Muito obrigado por todos os seus ensinamentos, paciência e por acreditar e investir em mim desde a minha graduação até o presente momento. O senhor não imagina o quanto contribuiu para o meu desenvolvimento profissional e humano, e o quanto eu sou grato por tudo isso!

Ao LOQuim. O melhor laboratório ever, com as melhores pessoas. Vocês foram fundamentais nesta minha etapa, me motivando a sempre buscar por mais nesse meio doido que é a academia, e a nunca desistir diante de um desafio. Obrigado mesmo, Talita (Talitis), Thayse, Keyla, Lucas, Thiago e Severino. Em especial à Josiane (Tia Josi), Jamerson (meu brother de BH, vulgo Bomba do Hemetério), Barbara (minha mãe acadêmica) e Felipe (meu brother, polícia e orientador), todo meu respeito e admiração por vocês!

Aos meus amigos do PPGO que convivi durante esse mestrado, especialmente Anne, Raqueline, Cibele, Malandro, Carol, Enatielly, Laís, Gabi, Lara, Andressa e Amanda Japa. Tenho uma consideração e um carinho gigante por vocês. Muito obrigado por todos os momentos que compartilhamos e vivemos durante esses dois anos, e que venham mais!

Aos meus grandes amigos. Meus biozueros da minha turma original, Anne, Amanda, Silmara, Fernando e Dayse, e os da turma que me adotou, Jaci, Duda, Jéssica, Ingrid, Paate e Lorena. Às minhas químicas, Karla e Bianca, e agora à nova integrante do grupo, a pequena coisa marlinda de tio, Gio! Foram nesses períodos pós conclusão dos cursos em que realmente descobri as pessoas com que quero continuar vivendo histórias ao lado. Muito obrigado pelos momentos de distração, diversão, e por ouvirem (aguentarem) meus desabafos por tanto tempo.

Aos funcionários e professores (com exceções) do PPGO, em especial à Dona Edileuza, André, Myrna, Tom, Rose, Ana, Professor Feitosa e Professora Doris.

Por fim, mas não menos importante, a CAPES, pela concessão da bolsa e financiamento do projeto. Afinal sem grana não haveria mestrado, então muito obrigado!

"Para mim é muito melhor entender o universo da forma que realmente é, do que persistir em um erro, ilusão, por mais gratificante e reconfortante que seja..."

Carl Sagan

## RESUMO

Na borda sudoeste do Oceano Atlântico tropical, caracterizada como oligotrófica, há áreas consideradas oásis, representadas pelas ilhas, atóis e montes submarinos. Os gradientes horizontes e verticais de velocidade induzidas a margem dessas feições geológicas promovem o aumento da turbulência e da biomassa do fitoplâncton próximas a elas, podendo alterar o sistema carbonato. O objetivo deste estudo é descrever a variabilidade vertical e interanual do sistema carbonato em torno do Arquipélago de Fernando de Noronha (AFN) e verificar como o processo de Efeito Ilha (EI) pode influenciar na sua distribuição. Dois transectos em lados opostos foram estabelecidos em torno do AFN de acordo com a direção do ramo central da Corrente Sul Equatorial. Amostras de água foram coletadas em julho de 2010, setembro de 2012 e julho de 2014, da superfície até os primeiros 500 m. Os resultados mostraram uma forte estratificação de densidade, com uma pequena elevação da estrutura termohalina a jusante da ilha durante 2010 e 2014. Os parâmetros do sistema carbonato foram fortemente correlacionados com a temperatura, a salinidade e oxigênio dissolvido ao longo da coluna de água e não alteraram significativamente entre os lados da ilha nos períodos estudados. Concluímos que o EI representado pelo aumento da biomassa do fitoplâncton a oeste da ilha não influenciou significativamente a variabilidade do sistema carbonato, que se mostrou mais correlacionada com o gradiente termohalino.

Palavras-chave: Efeito ilha. Carbono inorgânico. Processos turbulentos. Picnoclina.

## ABSTRACT

In the tropical, oligotrophic tropical Southwest Atlantic Ocean there are areas considered an oasis, represented by the islands, atolls and seamounts. The horizontal and vertical velocity gradients induced by the margin of these geological features promote the increase of the turbulence and the biomass of the phytoplankton around them, which can alter the carbonate system. The aim of this study is to describe the vertical and interannual variability of carbon chemistry around Fernando de Noronha Archipelago (FNA) and to verify how the Island Mass Effect (IME) process can influence on its distribution. Two transects on opposite sides were established in FNA according to the central branch of South Equatorial Current. Samples were collected in July 2010, September 2012 and July 2014, from the surface until the first 500m. The results showed a strong density stratification, with a small uplift of the thermohaline structure downstream the island during 2010 and 2014. The carbon chemistry parameters were strongly correlated with temperature, salinity and dissolved oxygen along the water column and did not change significantly between sides of the island in the studied periods. We concluded that the IME represented by the increase in phytoplankton biomass downstream the island did not influence on the carbon chemistry variability, which was more correlated with thermohaline gradient.

Keywords: Island mass effect. Inorganic carbon. Turbulent process. Pycnocline.

## LISTA DE ILUSTRAÇÕES

<b>Figura 1</b> - Ilustração do Efeito Ilha, com os principais processos e fontes que resultam no enriquecimento das águas entorno das ilhas. Fonte: Gove et al. (2016).....	15
<b>Figura 2</b> - Frações das espécies químicas inorgânicas do carbono em função do pH.....	17
<b>Figura 3</b> - Location of FNA (solid circle), the arrows indicate the directions of the currents, cSEC (solid arrow) and SEUC (dashed arrow). Sampling strategy around the island, 2010 cruise transect (red), 2012 (black) and 2014 (blue).....	22
<b>Figura 4</b> - Mean pycnocline in 2010 (a), 2012 (b) and 2014 (c) upstream (I) and downstream (II) FNA. Depth of 70m (red arrow), 85m (black arrow), and density isoline of $1.02388 \text{ kg L}^{-1}$ (blue arrow), $1.02383 \text{ kg L}^{-1}$ (green arrow) and $1.02357 \text{ kg L}^{-1}$ (yellow arrow).....	27
<b>Figura 5</b> - Temperature vs Salinity. Water masses, TSW (red dots) and SACW (black dots).....	28
<b>Figura 6</b> - Vertical distribution of chlorophyll-a in 2010 (a), 2012 (b) and 2014 (c) around FNA (in grey) on the SW transect (left-hand side of the island) and NE transect (right-hand side of the island).....	29
<b>Figura 7</b> - Comparison of TA linear regressions as a function of depth. Fits using the measured samples (red line), Equation 1 (black line), and using the relationship determined by Lee et al. (2006) (green line) and by Lefèvre et al. (2010) (blue line).....	30
<b>Figura 8</b> - Vertical distribution of calculated TA in 2010 (a), 2012 (b) and 2014 (c) around FNA (in grey) on the SW transect (left-hand side of the island) and NE transect (right-hand side of the island).....	31
<b>Figura 9</b> - Principal Component Analysis (PCA) of temperature ( $^{\circ}\text{C}$ ), salinity, [Chl-a], DO ( $\mu\text{mol kg}^{-1}$ ), DO%, DIP ( $\mu\text{mol kg}^{-1}$ ), DIN ( $\mu\text{mol kg}^{-1}$ ), Si(OH)4 ( $\mu\text{mol kg}^{-1}$ ), and measured TA ( $\mu\text{mol kg}^{-1}$ ) and CT ( $\mu\text{mol kg}^{-1}$ ).....	32
<b>Figura 10</b> - Comparison of CT linear regressions as a function of depth. Fits using the measured samples (red line), Equation 1 (black line), and using the relationship determined by Bonou et al. (2016) (blue dash line).....	32
<b>Figura 11</b> - Vertical distribution of calculated CT in 2010 (a), 2012 (b) and 2014 (c) around FNA (in grey) on the SW transect (left-hand side of the island) and NE transect (right-hand side of the island).....	33
<b>Figura 12</b> - Vertical distribution of $\Omega_{\text{ar}}$ in 2010 (a), 2012 (b) and 2014 (c) around FNA on the SW transect (left-hand side of the island) and NE transect (right-hand side of the island).....	34

## LISTA DE TABELAS

<b>Tabela 1</b> - Global Ocean Data Analysis Project Version 2 (GLODAPv2) data base used for Equation 2.....	26
<b>Tabela 2</b> - Average of nutrients according to depth and years around FNA. Western FNA ( <b>bold</b> and <i>italic</i> ), eastern FNA ( <i>italic</i> ).....	29

## LISTA DE ABREVIATURAS E SIGLAS

AAIW	Antarctic Intermediate Water
AFN	Arquipélago de Fernando de Noronha
ASPSP	Arquipélago de São Pedro e São Paulo
AT	Alcalinidade Total
B(OH) <sub>4</sub> <sup>-</sup>	Tetrahydroxyborate
C <sub>6</sub> H <sub>6</sub> O	Phenol
C <sub>6</sub> H <sub>8</sub> N <sub>2</sub> O <sub>2</sub> S	Sulfanilamide
CB	Corrente do Brasil
CCSE	Contracorrente Sul Equatorial
CG	Corrente da Guiné
Chl- <i>a</i>	Chlorophyll- <i>a</i>
CNB	Corrente Norte do Brasil
CRM	Certified Reference Materials
CSE	Corrente Sul Equatorial
cSEC	Central branch of South Equatorial Current
CFN	Cadeia de Fernando de Noronha
C <sub>T</sub>	Carbono Inorgânico Dissolvido Total
CTD	Conductivity-Temperature-Density
DCM	Deep Chlorophyll Maximum
DIN	Dissolved Inorganic Nitrogen
DIP	Dissolved Inorganic Phosphorus
DO	Dissolved Oxygen
DO%	Dissolved Oxygen Saturation
EI	Efeito Ilha
ENSO	El Niño Southern Oscillation
EPA	Environmental Protection Area
FNA	Fernando de Noronha Archipelago
GLODAPv2	Global Ocean Data Analysis Project Version 2

$H^+$	Hydrogen Proton
IME	Island Mass Effect
ITCZ	Intertropical Convergence Zone
N	North
NaClO	Hypochlorite
NADW	North Atlantic Deep Water
NE	Northeast
NECC	North Equatorial Countercurrent
$NH_3 + NH_4^+$	Nitrogênio Amoniacal
$NO_2^-$	Nitrite
$NO_3^-$	Nitrate
OMZ	Oxygen Minimum Zone
$pCO_2$	CO <sub>2</sub> Partial Pressure
pH	Potencial Hidrogeniônico
S	South
SACW	South Atlantic Central Water
SCSE	Subcorrente Sul Equatorial
SEUC	South Equatorial Under Current
$Si(OH)_4$	Silicate
SSS	Sea Surface Salinity
SST	Sea Surface Temperature
SW	Southwest
TA	Total Alkalinity
TSW	Tropical Surface Water
W	West
ZCIT	Zona de Convergência Intertropical
$\Omega_{ar}$	Taxa de Saturação de Aragonita

## SUMÁRIO

<b>1</b>	<b>INTRODUÇÃO .....</b>	<b>14</b>
1.1	APRESENTAÇÃO.....	14
1.2	ASPECTOS GERAIS.....	14
1.3	OBJETIVOS .....	19
1.3.1	<b>Objetivo Geral .....</b>	<b>19</b>
1.3.2	<b>Objetivos Específicos.....</b>	<b>19</b>
<b>2</b>	<b>CARBON CHEMISTRY VARIABILITY AROUND A TROPICAL ARCHIPELAGO .....</b>	<b>20</b>
2.1	INTRODUCTION .....	20
2.2	METHODS AND DATA .....	22
2.2.1	<b>Study Area.....</b>	<b>22</b>
2.2.2	<b>Sampling Strategy .....</b>	<b>23</b>
2.2.3	<b>Chemical Analyses.....</b>	<b>24</b>
2.2.3.1	Dissolved Oxygen and Dissolved Inorganic Nutrients .....	24
2.2.3.2	Total Alkalinity and Total Dissolved Inorganic Carbon .....	24
2.2.3.3	Aragonite Saturation.....	25
2.2.4	<b>Data Analyses.....</b>	<b>25</b>
2.2.5	<b>GLODAPv2 .....</b>	<b>25</b>
2.3	RESULTS .....	26
2.3.1	<b>Density (termohaline structure) .....</b>	<b>26</b>
2.3.2	<b>Chlorophyll-a and Nutrients .....</b>	<b>28</b>
2.3.3	<b>Total Alkalinity .....</b>	<b>30</b>
2.3.4	<b>Total Dissolved Inorganic Carbon .....</b>	<b>31</b>
2.3.5	<b>Aragonite Saturation.....</b>	<b>33</b>
2.4	DISCUSSION.....	34
2.5	CONCLUSIONS .....	37
<b>3</b>	<b>CONSIDERAÇÕES FINAIS.....</b>	<b>38</b>
	<b>REFERÊNCIAS .....</b>	<b>39</b>
	<b>APÊNDICE .....</b>	<b>49</b>

## 1 INTRODUÇÃO

### 1.1 APRESENTAÇÃO

Este documento de Dissertação está organizado em formato de artigo científico, considerando discussões sobre a variação das propriedades do sistema carbonato ou da química do carbono em torno de uma região insular, baseados em observações e coletas realizadas *in situ*. Pelo o que foi pesquisado até o presente momento, este é o primeiro estudo em regiões insulares que aborda essa temática.

Esta Dissertação apresenta-se em 3 capítulos: Este primeiro capítulo aborda um aspecto geral sobre a importância das regiões insulares, assim como sobre a caracterização do sistema carbonato e do Efeito Ilha, com ênfase no Oceano Atlântico Tropical, e os objetivos da presente pesquisa. O segundo capítulo apresenta o artigo intitulado *Carbon chemistry variability around a tropical archipelago* e submetido para a *Marine and Freshwater Research*, onde está descrito e discutido todos os resultados obtidos na presente pesquisa. Por fim, o terceiro capítulo aborda as considerações finais a respeito do tema trabalhado nesta dissertação.

O autor deste trabalho foi bolsista da Coordenação de Aperfeiçoamento de Pessoal de Nível Superior (CAPES), através do projeto Estudos sobre o ciclo do Carbono Inorgânico Dissolvido em áreas costeiras do Nordeste e Norte do Brasil e sua relação com os processos de acidificação oceânica (DICAM) financiado através do edital Ciências do Mar II/CAPES. As amostragens foram realizadas durante o projeto “Camadas Finas ao largo do Nordeste do Brasil”, com apoio da Diretoria de Hidrografia e Navegação e Ministério de Ciência, Tecnologia e Inovação - MCTI; e financiadas pelo projeto DICAM, com recursos CAPES/CMII.

### 1.2 ASPECTOS GERAIS

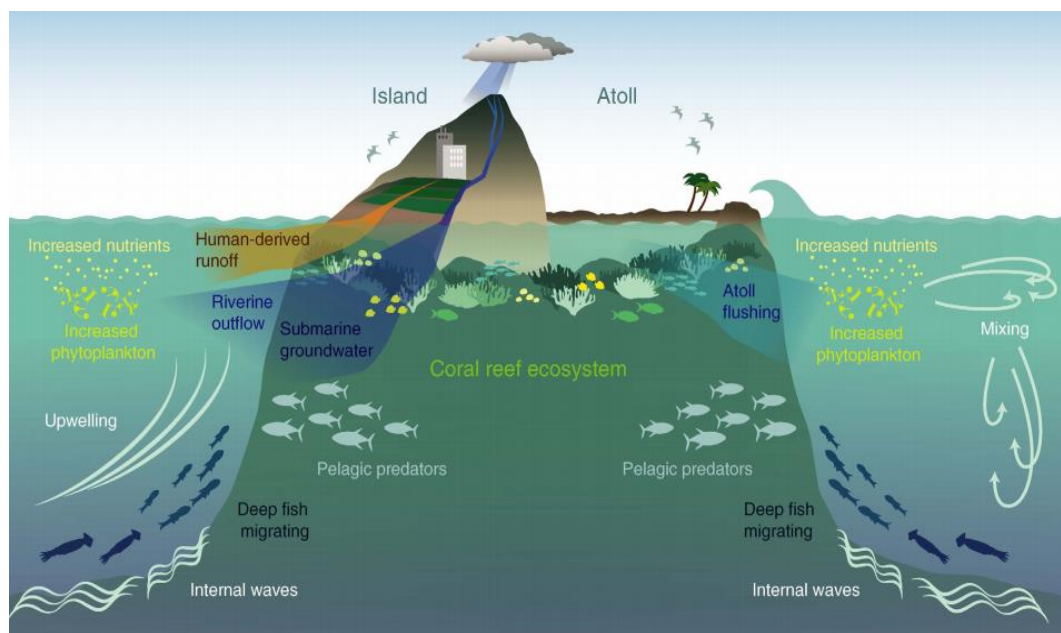
Os ambientes insulares são considerados *hotspots* de biodiversidade de organismos terrestres e marinhos, onde apresentam um elevado percentual de espécies endêmicas em consequência de seus espaços isolados e restritos à influência continental (SERAFINI et al., 2010; PINHEIRO et al., 2017). São formados a partir do extravasamento magmático da crosta oceânica, chegando a atingir a superfície, e representam cerca de 3% da cobertura terrestre global.

As ilhas oceânicas são consideradas verdadeiros “oásis” em meio a um deserto azul (oceano oligotrófico), com maiores concentrações de organismos planctônicos, que por sua vez influencia toda a teia trófica (LIMA et al., 2016). Isso se deve principalmente a um processo de

mesoescala denominado de Efeito Ilha (EI) (HASEGAWA et al., 2004; GOVE, 2005; TCHAMABI et al., 2017), que influencia as propriedades físicas, químicas e biológicas da água entorno dessas feições geológicas (SOUZA et al., 2013; GOVE et al., 2016).

O EI é representado pelo encontro de correntes marinhas e ventos com a topografia e orografia da ilha respectivamente (CALDEIRA et al., 2002; 2005). As correntes marinhas ao se “chocarem” com a topografia da ilha desencadeia um processo turbulento e de mistura na coluna d’água, que resulta na ascendência de águas mais profundas e promovem o aumento da concentração de nutrientes e da biomassa planctônica na camada superficial (DOTY & OGURI, 1956; CALDEIRA et al., 2002; HARLAN et al., 2002), conforme ilustrado na Figura 1. Esse processo varia de acordo com a velocidade da corrente, diâmetro da ilha, viscosidade e estratificação da água/vórtices formados, dentre outros fatores (HEYWOOD et al., 1990; 1996; CHANG et al., 2013; GOVE et al., 2016).

**Figura 1.** Ilustração do Efeito Ilha, com os principais processos e fontes que resultam no enriquecimento das águas entorno das ilhas. Fonte: Gove et al. (2016).



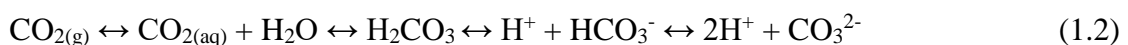
Já em relação aos ventos, a orografia da ilha pode bloquear seu fluxo, resultando também em uma mistura da coluna d’água (XIE et al., 2001), transporte vertical e horizontal de massas d’água, e principalmente em alterações positivas na temperatura superficial da água no lado abrigado da ilha (BASTERRETSEA et al., 2002; CALDEIRA et al., 2002). A intensidade desse processo é influenciada pela altura da área emersa da ilha, transporte de Ekman e pela velocidade dos ventos atuantes (BARTON, 2001; CALDEIRA et al., 2005; CHANG et al., 2013), sendo nesse caso também conhecido como Efeito Lee (BASTERRETSEA et al., 2002).

Estudos sobre o EI estão crescendo na comunidade científica, sendo a maioria até então concentrado no Oceano Pacífico (CALDEIRA et al., 2002; HASEGAWA et al., 2004; CALDEIRA et al., 2005; GOVE, 2005; TEAGUE et al., 2005; CHANG et al., 2013; ANDRADE et al., 2014; GOVE et al., 2016). O Oceano Pacífico apresenta cadeias de ilhas que são responsáveis pela fertilização da camada superficial em escala regional (GOVE et al., 2016), onde o EI pode ser influenciado diretamente por eventos climáticos como El Niño e La Niña, a partir de mudanças na intensidade de ventos e correntes (GOVE et al., 2006).

No Oceano Atlântico, a maioria dos estudos sobre EI estão compreendidos na região tropical (SOUZA et al., 2013; CORDEIRO et al., 2013; JALES et al., 2015; QUEIROZ et al., 2015; SILVA, 2016; TCHAMABI et al., 2017). Essa região, em geral, é caracterizada por águas superficiais com elevados valores de temperatura e salinidade, sendo uma das principais fontes de CO<sub>2</sub> para a atmosfera (TAKAHASHI et al., 2009; LEFÈVRE et al., 2010). Verticalmente apresenta uma forte estratificação de densidade, que resulta na diminuição da dispersão dos nutrientes dissolvidos na coluna d'água e consequentemente na atividade biológica (FLORES-MONTES, 2003).

Pesquisadores descrevem o EI como uma ressurgência de pequena escala (MACEDO et al., 1999). Diante disso, além de influenciar na teia trófica (LIRA et al., 2014; LIMA et al., 2016) e na concentração de nutrientes, esse processo pode desencadear alterações no sistema carbonato marinho a partir da ascendência de águas mais frias, ricas em CO<sub>2</sub> e pelo aumento da biomassa fitoplanctônica (LEFÈVRE et al., 2008).

O sistema carbonato marinho é representado pela dinâmica das espécies químicas inorgânicas do carbono a partir da dissolução do CO<sub>2</sub> atmosférico pelo processo de difusão. Uma vez em sua forma aquosa, o CO<sub>2</sub> se torna disponível para ser absorvido pela bomba biológica (Equação 1.1) e para reagir com a molécula da água (Equação 1.2):



A bomba biológica representa o consumo/liberação de CO<sub>2</sub> e nutrientes pelos organismos da comunidade primária, principalmente os fitoplanctons, para a realização dos processos metabólicos de fotossíntese e respiração (MILLERO, 2013). Em regiões oceânicas onde ocorre um aumento da produtividade e biomassa primária, como em áreas de ressurgência,

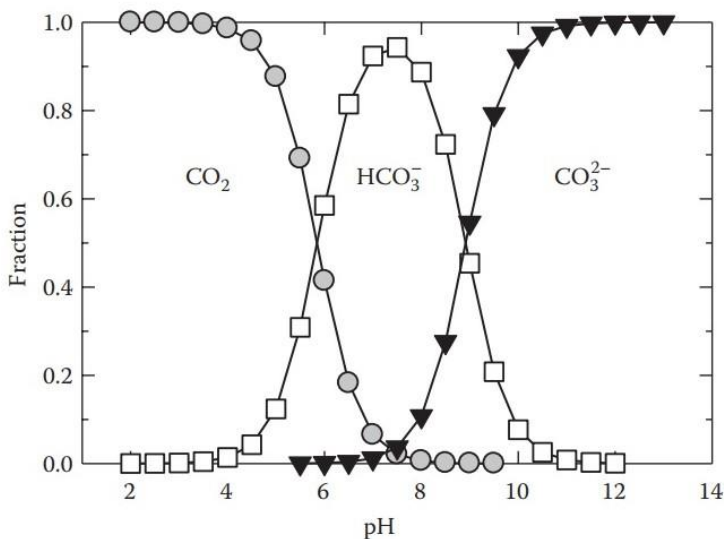
a intensificação do consumo de CO<sub>2</sub> pode influenciar significativamente no fluxo desse gás entre a interface oceano-atmosfera (TAKAHASHI et al., 2009).

Ao longo da coluna d'água, o processo fotossintético ocorre com maior intensidade no início da termoclinia, onde as concentrações de nutrientes são mais elevadas em comparação à superfície, e geralmente próximo à zona de 1% de luminosidade (FLORES-MONTES, 2003). Um dos produtos da fotossíntese é o carbono orgânico, que conforme atinge maiores profundidades, torna o CO<sub>2</sub> e os nutrientes disponíveis novamente através do processo de remineralização da matéria orgânica.

Uma vez em sua forma aquosa, o CO<sub>2</sub> reage com a molécula da água formando ácido carbônico (H<sub>2</sub>CO<sub>3</sub>), que se dissocia resultando na liberação de prótons (H<sup>+</sup>), bicarbonato (HCO<sub>3</sub><sup>-</sup>) e carbonato (CO<sub>3</sub><sup>2-</sup>) (Eq. 2.2). Mais de 90% do carbono oceânico se encontra na forma inorgânica, onde menos de 1% desse total é representado pelo CO<sub>2</sub>, cerca de 5% pelo CO<sub>3</sub><sup>2-</sup> e 94% pelo HCO<sub>3</sub><sup>-</sup> (MILLERO, 2013).

Em um perfil vertical a concentração dessas espécies químicas é regulada principalmente pelo pH. De acordo com a profundidade o pH tende a diminuir devido a maior disponibilidade de CO<sub>2</sub> e H<sup>+</sup>, oriundos do processo da remineralização da matéria orgânica (MILLERO, 2013). Conforme o pH é reduzido, o CO<sub>3</sub><sup>2-</sup> tende a reagir com os prótons livres para manter o equilíbrio químico do sistema, diminuindo assim sua concentração (Eq. 2.2). A Figura 2 ilustra o aumento/diminuição da fração desses compostos em relação ao pH.

**Figura 2:** Frações das espécies químicas inorgânicas do carbono em função do pH. Fonte: Millero (2013).



A dinâmica do sistema carbonato pode ser medida através de uma série de parâmetros como alcalinidade total (AT) e carbono inorgânico dissolvido total ( $C_T$ ). A AT representa o equilíbrio ácido/base ou a capacidade de tamponamento da água, sendo influenciada pelas concentrações de sais básicos, principalmente o  $HCO_3^-$  e  $CO_3^{2-}$  (DONEY et al., 2007; EGLESTON et al., 2010), conforme a equação:

$$AT = [HCO_3^-] + 2[CO_3^{2-}] + [B(OH)_4^-] + [OH^-] - [H^+] + \text{componentes menores} \quad (1.3)$$

Já o  $C_T$  representa o somatório de todas as espécies químicas inorgânicas do carbono:

$$C_T = [HCO_3^-] + [CO_3^{2-}] + [CO_2] \quad (1.4)$$

No Oceano Atlântico tropical, esses parâmetros são controlados principalmente por fatores físicos como temperatura, salinidade e correntes marinhas (BONOU et al., 2016; LEFÈVRE et al., 2016), podendo apresentar sazonalidade de acordo com a posição da Zona de Convergência Intertropical (ZCIT) (LEFÈVRE et al., 2010; 2013). Em relação às correntes, a Corrente Sul Equatorial (CSE) e Subcorrente Sul Equatorial (SCSE) são duas das que mais influenciam as águas superficiais e de subsuperfície da área respectivamente (STRAMMA & SCHOTT, 1999; STRAMMA et al., 2005).

A CSE é formada a partir da Corrente da Guiné (CG) no Oceano Atlântico tropical e apresenta três principais ramos, separados pela SCSE e pela Contracorrente Sul Equatorial (CCSE) (MOLINARI, 1982), onde seu ramo central se bifurca na Corrente Norte do Brasil (CNB) e na Corrente do Brasil (CB) (LUMPKIN & GARZOLI, 2005). Flui no sentido leste - oeste, transportando águas ricas em  $CO_2$  oriundas da divergência Equatorial (STRAMMA & SCHOTT, 1999; LEFÈVRE et al., 2008), com elevados valores de AT e  $C_T$  (BONOU, 2016). Já a SCSE é uma corrente considerada de subsuperfície na borda sudoeste do Oceano Atlântico tropical, que flui no sentido oposto ao da CSE. Influencia entre as latitudes de 3°S a 5 °S e transporta águas ricas em oxigênio oriundas da Subcorrente Norte do Brasil (SCNB) (STRAMMA & SCHOTT, 1999).

A borda sudoeste do Oceano Atlântico tropical vem sendo recentemente bastante estudada por apresentar particularidades que podem influenciar o sistema carbonato ou ciclo do carbono em nível regional (LEFÈVRE et al., 2010; 2017). A pluma do Rio Amazonas, como por exemplo, pode desencadear regiões de subsaturação de  $CO_2$ , e resultar em uma significativa redução da AT e  $C_T$  devido à intensa atividade biológica e ao aporte de água doce (BONOU et al., 2016; IBÁNHEZ et al., 2016; LEFÈVRE et al., 2017). Nessa região também encontra-se a

Cadeia de Fernando de Noronha (CFN) e o Arquipélago de São Pedro e São Paulo (ASPSP), áreas consideradas verdadeiros oásis em meio a um oceano oligotrófico (SOUZA et al., 2013).

O EI oriundo da CFN e ASPSP apresenta uma significativa influência na produtividade primária do Oceano Atlântico Sul tropical (CORDEIRO et al., 2013; QUEIROZ et al., 2015), contribuindo principalmente para o aumento da atividade pesqueira da região (HAZIN et al., 1998; LIMA et al., 2016). O presente trabalho buscou verificar a ocorrência do EI na ilha de maior destaque da CFN, o Arquipélago de Fernando de Noronha (AFN), e como esse processo influencia na distribuição dos parâmetros do sistema carbonato.

### 1.3 OBJETIVOS

#### 1.3.1 Geral

Caracterizar a distribuição vertical dos parâmetros do sistema carbonato e relacioná-la com variáveis físicas e biológicas na área em torno do Arquipélago de Fernando de Noronha (AFN).

#### 1.3.2 Específicos

Descrever a estrutura termohalina, a distribuição vertical clorofila-*a* e dos nutrientes inorgânicos dissolvidos da área de estudo.

Verificar a ocorrência do Efeito Ilha em torno do AFN a partir da descrição das propriedades físicas, químicas e biológicas analisadas e analisar sua influência sobre os parâmetros do sistema carbonato;

Elaborar equações para a determinação dos parâmetros do sistema carbonato em um perfil vertical.

## 2 CARBON CHEMISTRY VARIABILITY AROUND A TROPICAL ARCHIPELAGO

### 2.1 INTRODUCTION

The tropical Southwest Atlantic Ocean presents a significant role in the carbon dioxide ( $\text{CO}_2$ ) global dynamics as a strong source, due to the high values of temperature and salinity, and oligotrophic waters (TAKAHASHI et al., 2009; LEFÈVRE et al., 2010; BONOU et al., 2016). These waters properties vary horizontally and vertically according to several factors, such as the currents, waters masses and atmospheric conditions, creating a gradient of the carbon chemistry along the Atlantic Ocean (MILLERO et al., 1998; FEELY et al., 2004; LEE et al., 2006; KITIDIS et al., 2016).

In a horizontal gradient, the surface area is influenced specially by the South Equatorial Current (SEC) (LEFÈVRE et al., 2013; TCHAMABI et al., 2017). The SEC flows from the Southeast to the Tropical Southwest Atlantic Ocean (STRAMMA & SCHOTT, 1999; RODRIGUES et al., 2007), transporting saturated  $\text{CO}_2$  waters (LEFÈVRE et al., 2010; LEFÈVRE et al., 2013).

The SEC and the South Equatorial Under Current (SEUC) influence the water column from the surface to around the first 500m (STRAMMA & ENGLAND, 1999), transporting two water masses, the Tropical Surface Water (TSW) and the South Atlantic Central Water (SACW) in subsurface waters (STRAMMA & ENGLAND, 1999; SILVA et al., 2005; ASSUNÇÃO et al., 2016). In a vertical distribution, the TSW is represented by the maximum temperature/salinity values, creating a strong thermohaline stratification. This stratification blocks the vertical transport of dissolved nutrients, limiting the primary productivity in the region (JALES et al., 2015; QUEIROZ et al., 2015). Due to this oligotrophy, carbon chemistry is controlled mainly by physical processes (GONZÁLES-DÁVILA et al., 2010; LEFÈVRE et al., 2017).

Nevertheless, studies have been registering physical, chemical and biological alterations, specially at the primary community, in areas where there is a disruption or uplift of the thermohaline structure (SOUZA et al., 2013; ANDRADE et al., 2014; GOVE et al., 2016). This is promoted by the presence of islands and seamounts. The island acts as a barrier to wind and marine current flow, which can create wakes usually at its lee side (CHANG et al., 2013). Winds wakes are related specially with the sea surface temperature (SST) changes, due to the sheltering from island's orography (CALDEIRA et al., 2002; 2005), while marine currents

wakes are caused by the disturbance of water with the island's topography (COUTIS & MIDDLETON, 2002; TCHAMABI et al., 2017).

Areas surround islands are considered “oasis” in an oligotrophic environment, presenting an increase at biological productivity and fishing activities (JALES et al., 2015; CORDEIRO et al., 2013; SOUZA et al., 2013). This is due the “island mass effect” (IME) process, first described by Doty & Oguri (1956), associated to the currents wakes (CHANG et al., 2013).

The currents wakes create eddies vortices at the leeward side of the island, which increase the mixing rate, and take deep nutrients and CO<sub>2</sub>-rich waters to surface (small-scale upwelling), promoting the biological increase (GOVE et al., 2016). The capacity of the eddies vortices is controlled by several factors such as the currents intensity, island diameter, the surrounding depth and the creation of internal waves (CALDEIRA & MARCHESIELLO, 2002; ZHENG & ZHENG, 2004; GOVE et al., 2006; HASEGAWA et al., 2014).

Biological activity is mainly represented by the plankton community in ocean areas, playing an essential role on carbon dynamics along the water column (PIONTKOVSKI et al., 2003). During periods of upwelling in the Tropical Atlantic the carbonate system is controlled specially by these organisms (LEFÈVRE et al., 2008), and the occurrence of the IME is considered an important mechanism that contributes with the average biological productivity of the region (HARLAN et al., 2002; SOUZA et al., 2013; JALES et al., 2015; GOVE et al., 2016).

At western of the tropical South Altantic Ocean there is the Fernando de Noronha Ridge (FNR), a chain represented by an atoll, islands and seamounts (ALMEIDA, 2006). Studies performed across this area have been showing that the central branch of SEC (cSEC) is disrupted by the islands topographies, and results in the increase of phytoplankton and zooplankton community (CORDEIRO et al., 2013; SOUZA et al., 2013; LIRA et al., 2014; QUEIROZ et al., 2015; LIMA et al., 2016; TCHAMABI et al., 2017). Fernando de Noronha Archipelago (FNA) is the largest island from the ridge and the only one populated, which is also a factor that influence in the IME and the carbon chemistry, by adding nearshore nutrients and organic matter (GOVE et al., 2016).

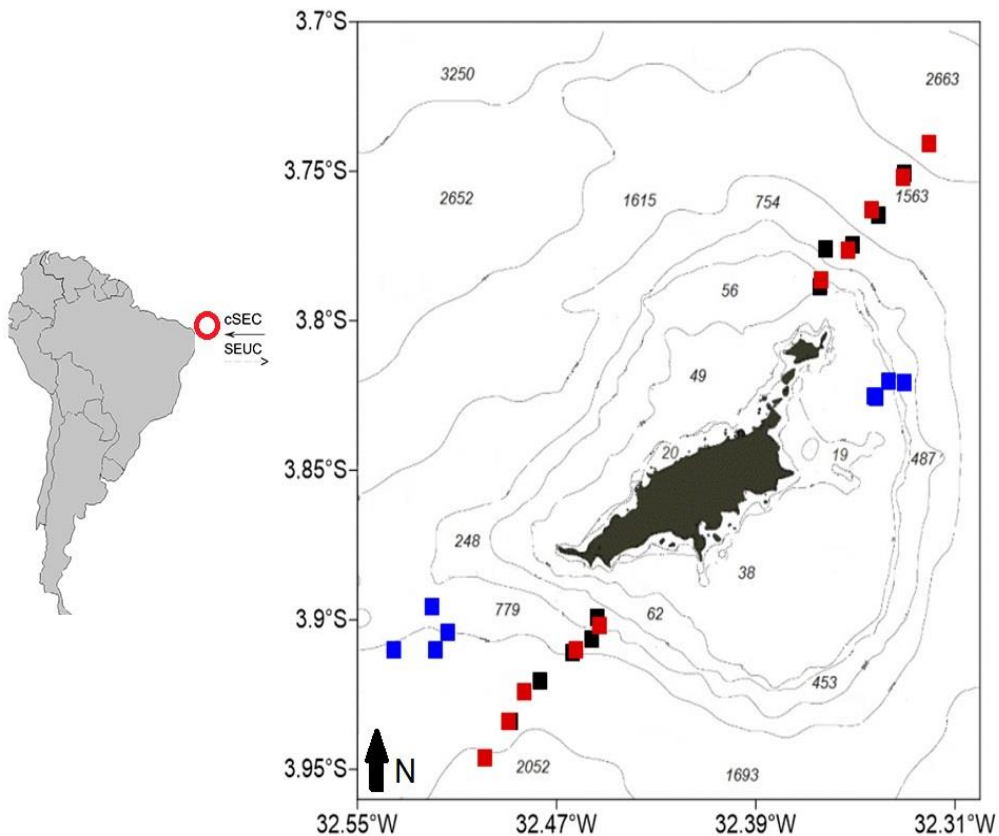
This study aims to verify the occurrence of the IME around FNA by describing the density structure, chlorophyll-*a* and nutrients distribution, and as researched by far, is the first to investigate how the IME can influence on the carbon chemistry and to describe the interannual vertical distribution of these parameters in a tropical region.

## 2.2 METHODS AND DATA

### 2.2.1 Study Area

The FNA is located at the tropical Southwest Atlantic Ocean ( $3^{\circ}51' S$ ,  $32^{\circ}25' W$ ), at approximately 360km offshore Brazil Northeast (Fig. 3). It presents an area of  $20\text{km}^2$  represented by one main island that occupies 91% of the total area of the archipelago, and 20 islets and rocks (Fig. 3). FNA is considered a marine national park and an Environmental Protection Area (EPA) due to its importance in the biodiversity maintenance, being local of some endemic species (SAMPAIO et al., 2004; LIRA et al., 2014).

**Figure 3:** Location of FNA (solid circle), the arrows indicate the directions of the currents, cSEC (solid arrow) and SEUC (dashed arrow). Sampling strategy around the island, 2010 cruise transect (red), 2012 (black) and 2014 (blue).



The island is part of a seamounts chain originated by volcanic activity, with its base in a depth of 4.000m (ALMEIDA, 2006). During its formation, the rocks of FNA were covered by alkaline basaltic lava (MARQUES et al., 2007) and the sediments are predominantly sandy moderately sorted and bioclastic, with high carbonate fraction (>90%) at the coastal areas (BARCELLOS et al., 2017).

The climate is typically tropical, with a defined rainy (between March and July) and dry (August to February) season. The water column around the FNA is represented by four main water masses: TSW, characterized by the mixed layer of Atlantic, with temperatures of about 27°C and maximum salinities; South Atlantic Central Water (SACW), represented by linear relationships between temperature and salinity; Antarctic Intermediate Water (AAIW), identified by the minimum values of salinity; North Atlantic Deep Water (NADW), the deeper water mass, between 1200m and 4000m, represented by the minimum temperatures (STRAMMA & SCHOTT, 1999; STRAMMA & ENGLAND, 1999; SILVA et al., 2005).

Surface water is influenced specially by the southeastern trade winds and the central branch of the South Equatorial Current (cSEC), while subsurface water is impacted by the South Equatorial Under Current (SEUC) (REVERDIN et al., 1991). The cSEC is fed by the recirculation of the North Equatorial Countercurrent (NECC), the equatorial upwelling and by the Guinea Current (LUMPKIN & GARZOLI, 2005). At the western basin of Atlantic Ocean, the cSEC presents strongest periods during the austral winter, reaching  $0.35 \text{ m s}^{-1}$  of velocity (TCHAMABI et al., 2017).

The SEUC is considered a subthermocline current, fed by the equatorial and south branch of SEC flow, transporting an oxygen-rich water westward (STRAMMA & SCHOTT, 1999). This current also presents strongest periods during the austral winter (REVERDIN et al., 1991), with an average velocity of  $0.2 \text{ m s}^{-1}$  and a vertical extension from 200m to 500m (SCHOTT et al., 2003).

### **2.2.2 Sampling Strategy**

At board of the research vessel NHOc38 Cruzeiro do Sul, three cruises were performed around the FNA, one in 2010 (July – rainy season), 2012 (September – dry season) and 2014 (July – rainy season), where in each year two transects were established (northeast (NE) and southwest (SW) side of the island) according to the direction and intensity of the cSEC (Fig. 3).

A rosette with 5L Niskin bottles was used to collect discrete water samples, and a Conductivity-Temperature-Density (CTD) Seabird 911plus® was used to provide real-data collection along the water column until 500m, with auxiliary sensors (dissolved oxygen (DO), pH and fluorescence). The water samples were collected at the surface, deep chlorophyll maximum (DCM), upper, middle and the base of thermocline and oxygen minimum zone (OMZ), and were measured DO, dissolved inorganic nutrients and the carbonate parameters.

### **2.2.3 Chemical Analyses**

#### **2.2.3.1 Dissolved Oxygen and Dissolved Inorganic Nutrients**

Dissolved oxygen (DO) was measured on board by the modified method of Winkler (STRICKLAND & PARSONS, 1972). Its saturation (DO%) was calculated according to the International Oceanographic Tables (UNESCO, 1973).

The dissolved inorganic nutrients were measured through colorimetric methods using a spectrophotometer Cary 100. Ammonium ( $\text{NH}_3+\text{NH}_4^+$ ) was measured following Grasshoff et al. (1983), consisted in the blue indophenol formed by the reaction of phenol ( $\text{C}_6\text{H}_6\text{O}$ ) and sodium hypochlorite ( $\text{NaClO}$ ) with  $\text{NH}_3+\text{NH}_4^+$ . Nitrate ( $\text{NO}_3^-$ ) and nitrite ( $\text{NO}_2^-$ ) were measured by the sulfanilamide ( $\text{C}_6\text{H}_8\text{N}_2\text{O}_2\text{S}$ ) method (STRICKLAND & PARSONS, 1972). Dissolved inorganic nitrogen (DIN) was represented by the sum of  $\text{NO}_3^-$ ,  $\text{NO}_2^-$  and  $\text{NH}_3+\text{NH}_4^+$  concentrations. Silicate ( $\text{Si}(\text{OH})_4$ ) and the dissolved inorganic phosphorus (DIP) were determined based on the reactions of orthosilicic acid and ions phosphate ( $\text{PO}_4^{3-}$ ) respectively with acidified molybdate, reduced to a blue compound (GRASSHOFF et al., 1983).

#### **2.2.3.2 Total Alkalinity and Total Dissolved Inorganic Carbon**

Carbonate parameters samples were poisoned with mercury chloride ( $\text{HgCl}_2$ ) to prevent biological alteration. TA ( $n = 6$ ) and  $C_T$  ( $n = 6$ ) from 2012 cruise were measured by potentiometric titration in a closed cell (EDMOND, 1970) with the equivalent points calculated following the method described by Dickson and Goyet (1994). While TA samples from 2014 cruise ( $n = 15$ ) were used the Dickson et al. (2007) methodology.

Certified Reference Materials (CRM) provided by Andrew Dickson (Scripps Institutions of Oceanography, San Diego, USA) were utilized for calibration and validation of the values, with an accuracy of 99.88% and an uncertainty of 2.53 and 1  $\mu\text{mol kg}^{-1}$  for TA and  $\text{C}_\text{T}$  respectively.

#### 2.2.3.3 Aragonite Saturation

Aragonite ( $\Omega_{\text{ar}}$ ) saturation values were calculated by the CO2SYS software®. It was used the calculated TA and  $\text{C}_\text{T}$ , salinity, temperature, and the carbonic acid dissociation constants of Mehrbach et al. (1973), refitted by Dickson and Millero (1987), in the calculations. It was calculated by  $\Omega = [\text{Ca}^{+2}] [\text{CO}_3^{2-}] / K'_{\text{sp}}$ , where the  $[\text{Ca}^{+2}]$  is the calcium concentration and  $K'_{\text{sp}}$  is the apparent solubility of the mineral. Values  $> 1$  represents saturate conditions (FEELY et al., 2009).

#### 2.2.4 Data Analyses

It was used the Analysis of Variance (ANOVA) to test the effect of interannual variation and transects or sides of the island on the density, chlorophyll-*a*, TA and  $\text{C}_\text{T}$  values, with an  $\alpha$  of 0.05. Principal Components Analysis was used to explain the correlations between all the measured variables.

#### 2.2.5 GLODAPv2

Since the sampling for  $\text{C}_\text{T}$  happened only in 2012 cruise, with the aim to do a better temporal evaluation, the Global Ocean Data Analysis Project Version 2 (GLODAPv2) data base from stations next to FNA (Table 1) were added to the results.

The GLODAPv2 represents a combined of open data from oceanographic campaign preformed all over the world, such as the CARINA (Carbon in the Atlantic), PACIFICA (Pacific Interior Ocean Carbon), GEOSECS (Geochemical Section Study) and others, with a total of 724 cruises over 40 years. Its main aim is to generate a unified data set to describe how anthropogenic and natural inorganic carbon have changed and is currently influencing the world ocean.

Along the years it was observed an improvement of the results specially for the carbon chemistry, where the precision of the  $C_T$  measurement is around  $4 \mu\text{mol kg}^{-1}$  and for TA is around  $3 \mu\text{mol kg}^{-1}$  (OLSEN et al., 2016). GLODAPv2 is an unique and quality-controlled data product, and this is proved by the consistency of the parameters (SABINE et al., 2005; OLSEN et al., 216).

**Table 1:** Global Ocean Data Analysis Project Version 2 (GLODAPv2) data base used for Equation 2.

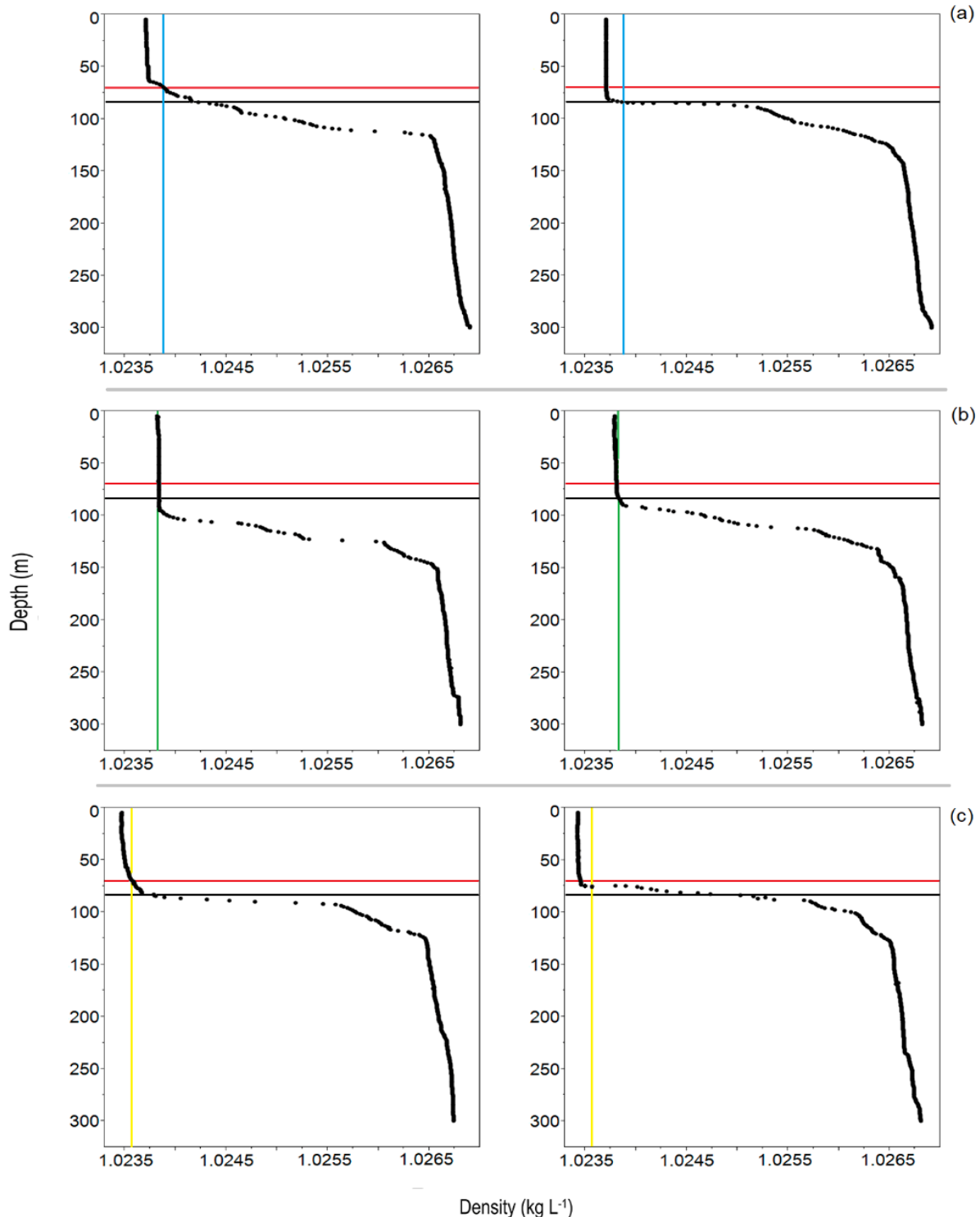
Cruise	Station (coordinates)	Year
	59 (3.002°S, 35.008°W)	
334 (n = 16)	60 (3.499°S, 34.909°W)	1996
	61 (3.963°S, 35.004°W)	
	17 (3.999°S, 35°W)	
389 (n = 36)	18 (3.491°S, 34.889°W)	1999
	19 (3°S, 35.001°W)	
61 (n = 30)	5 (4.003°S, 34.884°W)	2006
	7 (3.005°S, 34.885°W)	
235 (n = 42)	69 (4.198°S, 30.068°W)	2013
	70 (3.105°S, 29.982°W)	

## 2.3 RESULTS

### 2.3.1 Density (thermohaline structure)

The vertical distribution of density was represented by a stratification, with less dense waters at the surface, increasing the values along the depth. The density varied from  $1.0234 \text{ kg L}^{-1}$  to  $1.0269 \text{ kg L}^{-1}$ , with the lowest surface value in 2014 (Fig. 4). It was observed a deep pycnocline from 70m to  $\sim 140\text{m}$ . Also, it was registered a subsurface water rising downstream FNA, with the isoline of  $1.02388 \text{ kg L}^{-1}$  in 70m upstream and in 85m downstream during 2010 cruise (Fig. 4a), and the isoline of  $1.02357 \text{ kg L}^{-1}$  in 70m at lee side and in  $\sim 80\text{m}$  eastern the island during 2014 cruise (Fig. 4c).

**Figure 4:** Mean pycnocline in 2010 (a), 2012 (b) and 2014 (c) upstream (right-hand side) and downstream (left-hand side) FNA. Depth of 70m (red line), 85m (black line), and density isoline of  $1.02388 \text{ kg L}^{-1}$  (blue line),  $1.02383 \text{ kg L}^{-1}$  (green line) and  $1.02357 \text{ kg L}^{-1}$  (yellow line).

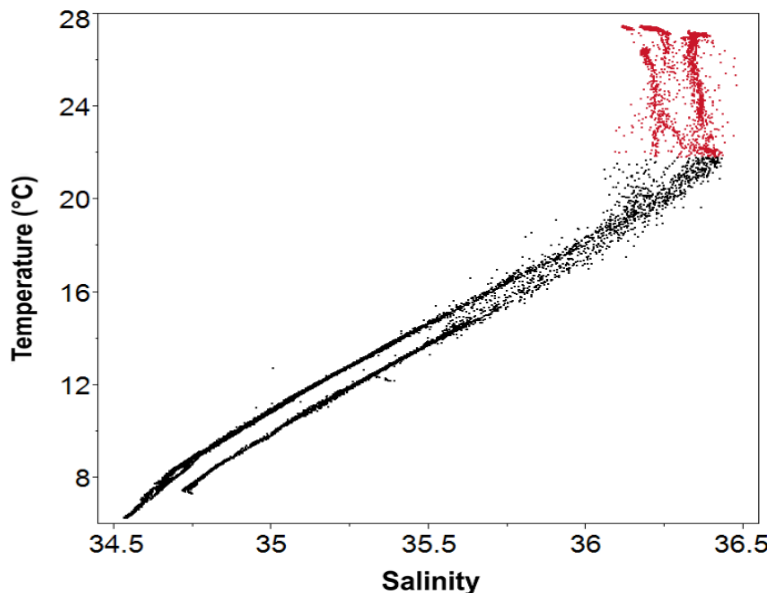


Temperature presented positive strong correlations ( $r^2 > 0.9$ ) with salinity and DO, and strong negative correlations ( $r^2 < -0.9$ ) with DIN and DIP. Salinity presented positive strong

correlation ( $r^2 > 0.9$ ) with the DO, also negative relationships ( $r^2 < -0.9$ ) with DIN and DIP (Fig. 9). There were no significant differences in the density between the years and sides of the island ( $p > 0.1$ ).

The TSW was present from the surface until upper pycnocline (~90m), while the SACW was from the thermocline until 500m (Figure 5).

**Figure 5:** Temperature vs Salinity. Water masses, TSW (red dots) and SACW (black dots).



### 2.3.2 Chlorophyll-a and Nutrients

Concentration of chlorophyll-*a* ([Chl-*a*]) varied from  $1.21 \text{ mg m}^{-3}$  to  $0.01 \text{ mg m}^{-3}$ , with the highest values registered in 2010 (Fig. 6). The Deep Chlorophyll Maxima (DCM) was at the base of photic layer (~90m), decreasing the concentration along the depth. The values varied significantly between years, and sides of the island during 2010 and 2014 cruises ( $p < 0.1$ ), where it was observed an increase at the west side of FNA (Fig. 6a, c). [Chl-*a*] presented a positive correlation ( $r^2 > 0.6$ ) with the temperature and salinity, and a negative one ( $r^2 < -0.5$ ) with the DIN and DIP in 2010 and 2014. During 2012 cruise there was no significant correlations with [Chl-*a*].

The vertically distribution of nutrients was represented by low values at the photic layer, increasing along the depth (Table 2). During 2010 and 2014 cruises, the surface concentrations of DIN and DIP were higher than at DCM western the island. DIN and DIP presented strong negative correlations ( $r^2 < -0.85$ ) with TA and DO, and strong positive ( $r^2 > 0.9$ ) with C<sub>T</sub> (Fig. 9). These values were not significantly different ( $p > 0.1$ ) between the sides of FNA and the years.

**Figure 6:** Vertical distribution of chlorophyll-a in 2010 (a), 2012 (b) and 2014 (c) around FNA (in grey) on the SW transect (left-hand side of the island) and NE transect (right-hand side of the island).

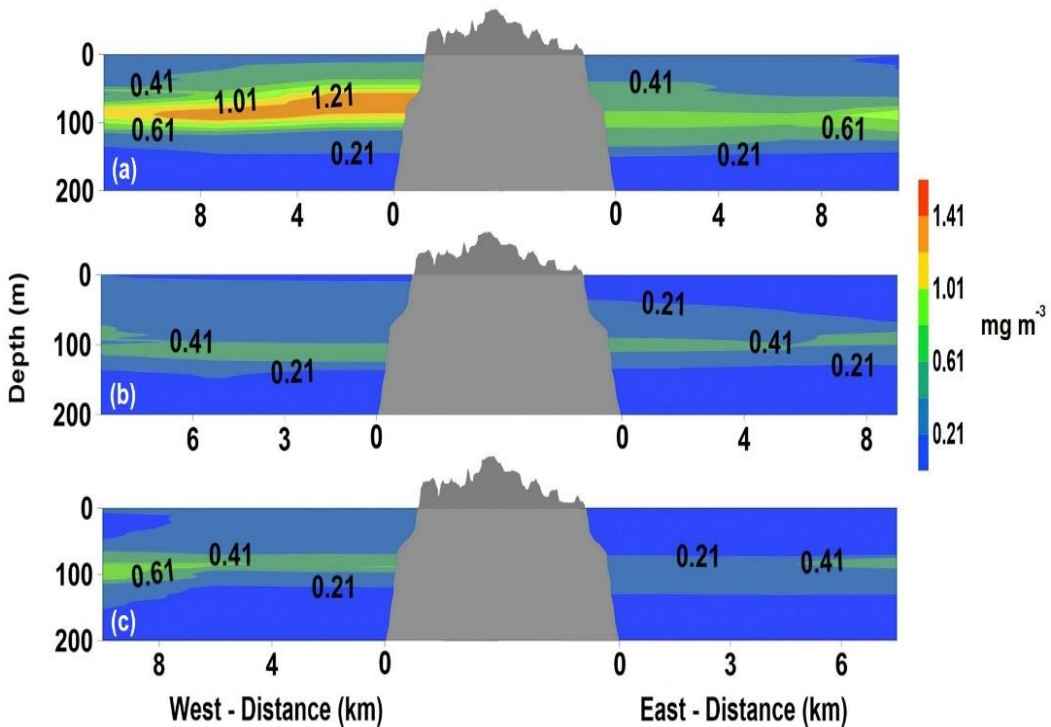


**Table 2:** Average of nutrients according to depth and years around FNA. Western FNA (**bold** and *italic*), eastern FNA (*italic*).

Parameters	Years						Depth
	2010	2012	2014	2010	2012	2014	
<b>Western FNA</b>				Eastern FNA			
	<b>2.39</b>	<i>1.25</i>	<b>0.73</b>	0.80	<i>1.38</i>	<b>0.35</b>	Surface (2m)
DIN	<b>1.57</b>	<i>5.08</i>	<b>0.46</b>	2.81	2.64	<i>1.82</i>	DCM (~100m)
(μmol L⁻¹)	<b>6.83</b>	<i>9.40</i>	<b>1.75</b>	5.82	<i>10.77</i>	<b>3.91</b>	Middle of Pycnocline (~120m)
	<b>19.06</b>	<i>15.22</i>	<b>8.27</b>	14.98	<i>15.06</i>	<b>10.03</b>	Pycnocline base (~150m)
<b>0.17</b>						Surface (2m)	
DIP	<b>0.14</b>	<i>0.26</i>	<b>0.16</b>	0.31	0.15	<i>0.20</i>	DCM (~100m)
(μmol L⁻¹)	<b>0.50</b>	<i>0.38</i>	<b>0.24</b>	0.54	0.75	<i>0.49</i>	Middle of Pycnocline (~120m)
	<b>1.01</b>	<i>0.69</i>	<b>0.75</b>	1.15	1.14	<i>1.09</i>	Pycnocline base (~150m)

### 2.3.3 Total Alkalinity

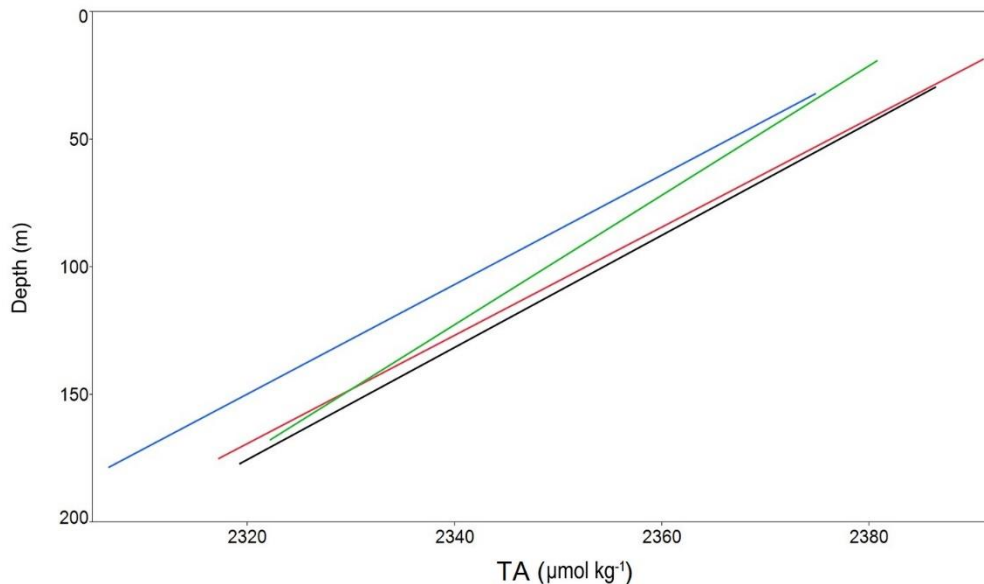
The measured TA samples from all the cruises ( $n = 21$ ) presented strong positive correlations ( $r^2 > 0.9$ ) with temperature ( $^{\circ}\text{C}$ ), salinity, DO and its saturation (DO%), and negative ( $r^2 < -0.9$ ) with  $\text{C}_\text{T}$  (Fig. 9). The values were not significantly different between the years and sides of the island ( $p > 0.1$ ), and this allowed the determination of a linear regression (Equation 2.1) for a better interannual evaluation along the water column:

$$\text{TA} = -28.78 + (-1.70 \times \text{Temperature}) + (67.13 \times \text{Salinity}) + (0.23 \times \text{DO}\%) \quad r^2 = 0.95$$

Eq. (2.1)

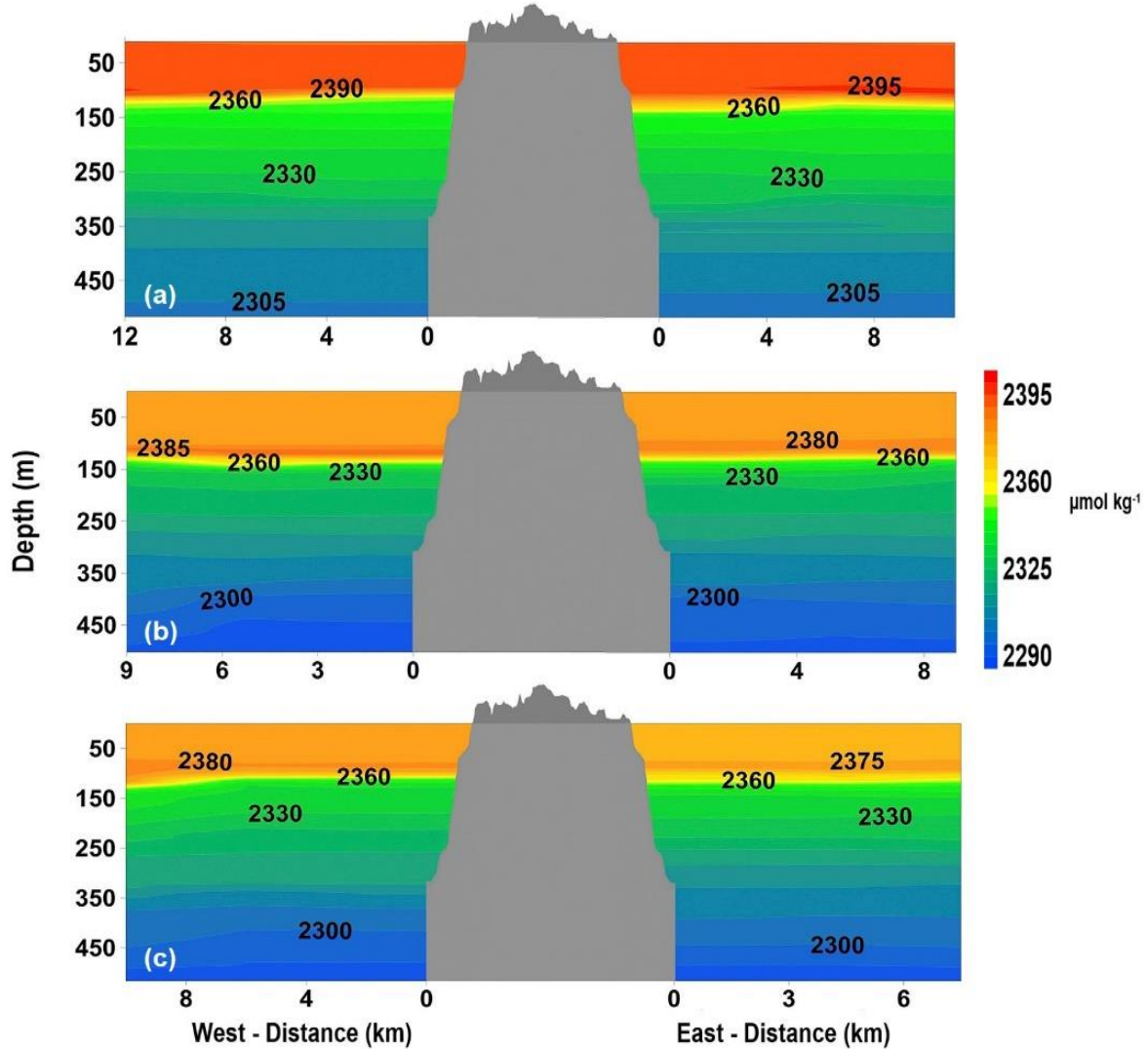
TA calculated using Eq. (2.1) presented an error of  $\pm 1.35 \mu\text{mol kg}^{-1}$ , while by using regressions for surface TA calculation proposed by Lefèvre et al. (2010) and Lee et al. (2006) differed  $\pm 9.81 \mu\text{mol kg}^{-1}$  and  $\pm 5.42 \mu\text{mol kg}^{-1}$  respectively. Figure 7 shows the comparison of these linear regressions as a function of depth.

**Figure 7:** Comparison of TA linear regressions as a function of depth. Fits using the measured samples (red line), Equation 1 (black line), and using the relationship determined by Lee et al. (2006) (green line) and by Lefèvre et al. (2010) (blue line).



TA calculated followed the salinity stratification (Fig. S1), concentrated at the subsurface and decreasing along the depth (Fig. 8). These values varied from  $2398.22 \mu\text{mol kg}^{-1}$  at the surface to  $2282.72 \mu\text{mol kg}^{-1}$  in  $\sim 500\text{m}$ , with the highest surface value registered in 2010 (Fig. 8a).

**Figure 8:** Vertical distribution of calculated TA in 2010 (a), 2012 (b) and 2014 (c) around FNA (in grey) on the SW transect (left-hand side of the island) and NE transect (right-hand side of the island).



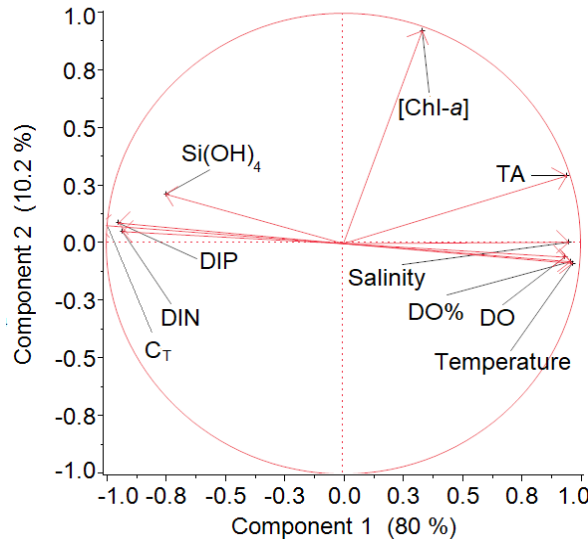
#### 2.3.4 Total Dissolved Inorganic Carbon

$C_T$  samples measured experimentally ( $n = 6$ ) presented strong negative relationships ( $r^2 < -0.9$ ) with salinity, temperature ( $^{\circ}\text{C}$ ) and DO ( $\mu\text{mol kg}^{-1}$ ), and positive ( $r^2 > 0.9$ ) with nutrients, as it is possible to visualize in the figure 9. Figure 9 shows clearly the correlations between the measured parameters, with the component 1 explaining 80% of the variation along de depth, while component 2 explain 10.2% represented by the variation between years. Temperature, salinity and DO were strongly correlated with TA and  $C_T$  during all cruises.

It was added the  $C_T$  values from GLODAPv2 ( $n = 124$ ), which also presented significant correlations with salinity, temperature ( $^{\circ}\text{C}$ ) and DO ( $\mu\text{mol kg}^{-1}$ ), and allowed the creation of an empirical regression (Equation 2.2):

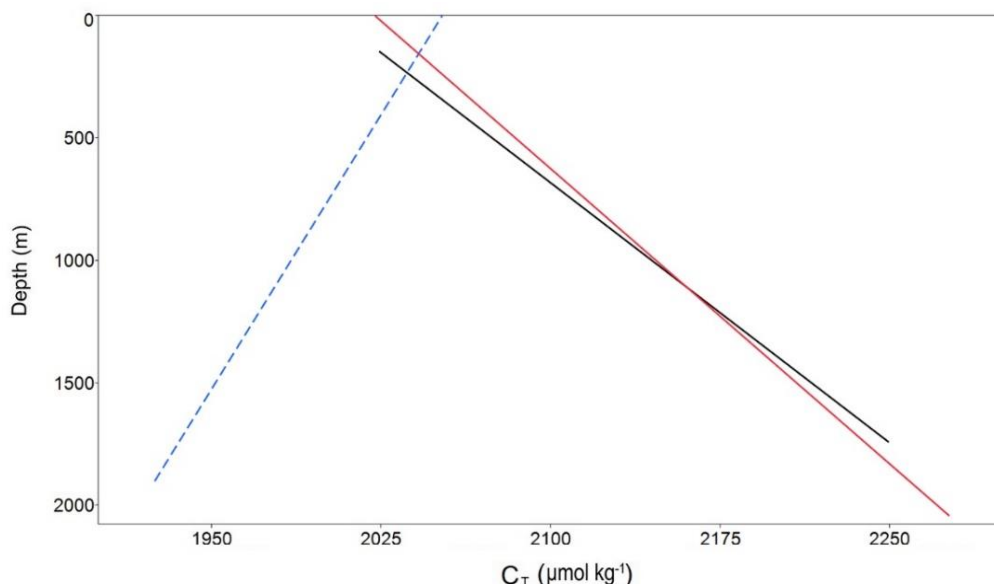
$$C_T = 771.44 + (0.73 * \text{Year}) + (2.83 * \text{Salinity}) + (-6.65 * \text{Temperature}) + (-0.54 * \text{DO}) \\ r^2 = 0.88 \quad \text{Eq. (2.2)}$$

**Figure 9:** Principal Component Analysis (PCA) of temperature ( $^{\circ}\text{C}$ ), salinity, [Chl-*a*], DO ( $\mu\text{mol kg}^{-1}$ ), DO%, DIP ( $\mu\text{mol kg}^{-1}$ ), DIN ( $\mu\text{mol kg}^{-1}$ ), Si(OH)<sub>4</sub> ( $\mu\text{mol kg}^{-1}$ ), and measured TA ( $\mu\text{mol kg}^{-1}$ ) and C<sub>T</sub> ( $\mu\text{mol kg}^{-1}$ ).



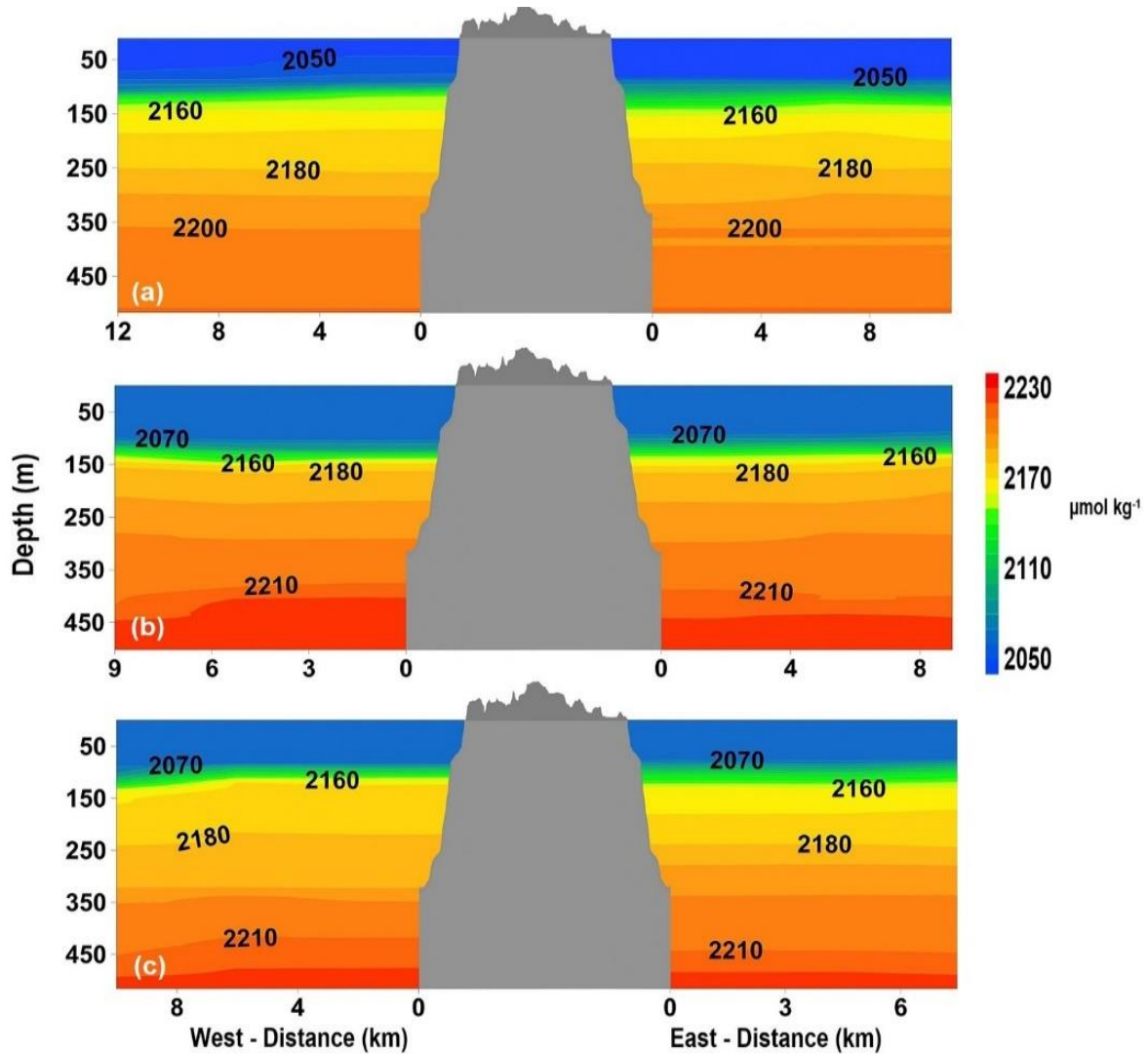
C<sub>T</sub> calculated using Eq. (2.2) presented an error of  $\pm 4.07 \mu\text{mol kg}^{-1}$ , while by using the regression for surface C<sub>T</sub> calculation proposed by Bonou et al. (2016), which was adapted from Lefèvre et al. (2010) and considered just salinity, the values presented an error of  $\pm 213.45 \mu\text{mol kg}^{-1}$ . Figure 10 shows the comparison of these linear regressions as a function of depth.

**Figure 10:** Comparison of C<sub>T</sub> linear regressions as a function of depth. Fits using the measured + GLODAPv2 samples (red line), Equation 1 (black line), and using the relationship determined by Bonou et al. (2016) (blue dash line).



Using Eq. (2.2)  $C_T$  varied from  $2229 \mu\text{mol kg}^{-1}$  to  $2045 \mu\text{mol kg}^{-1}$  (Fig. 11), and presented a negative correlation with chlorophyll-a ( $r^2 < -0.6$ ) in 2010 and 2014. The photic layer was represented by the minimum values, with the lowest surface value registered in 2010, increasing along the depth (Fig. 11a).

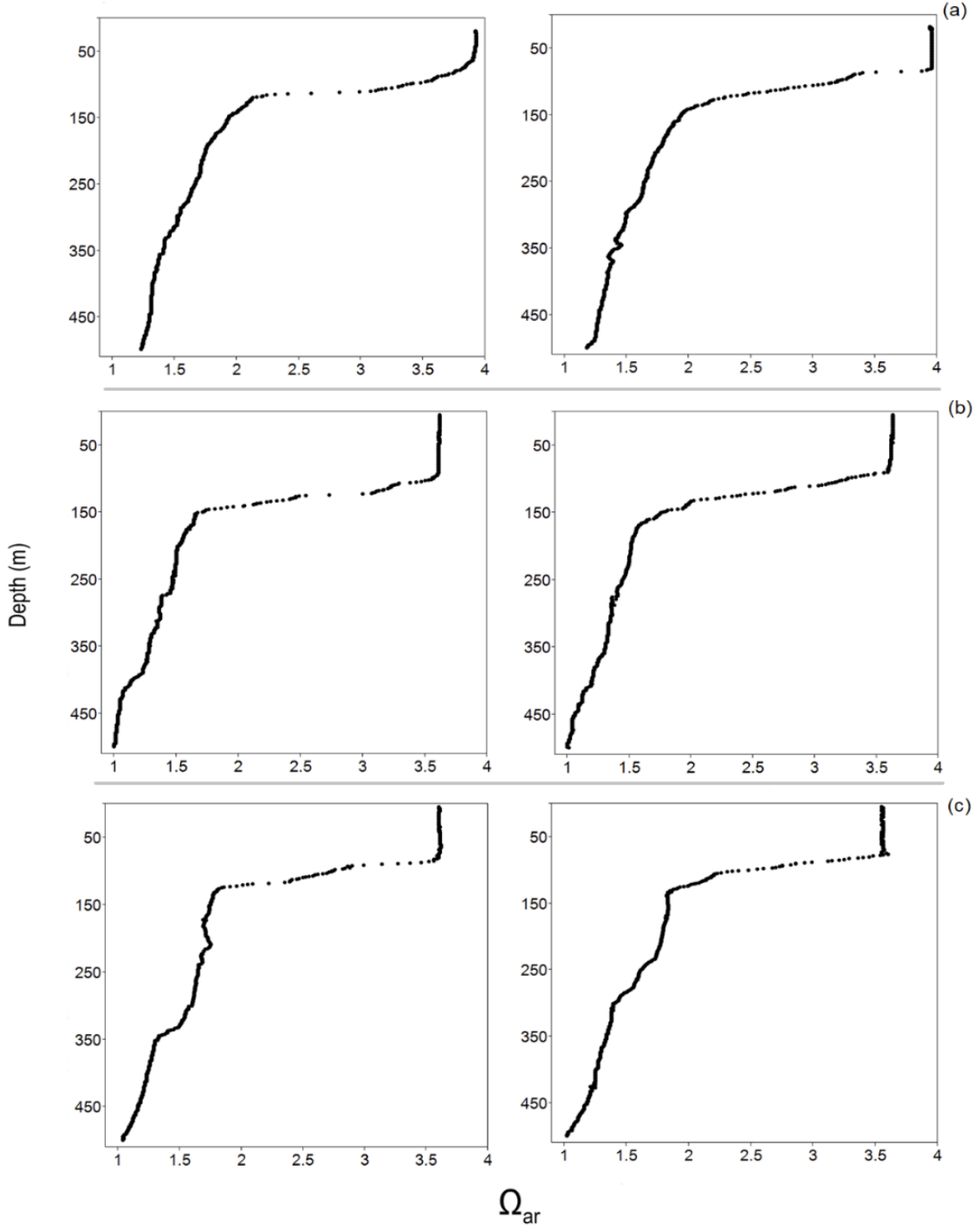
**Figure 11:** Vertical distribution of calculated  $C_T$  in 2010 (a), 2012 (b) and 2014 (c) around FNA (in grey) on the SW transect (left-hand side of the island) and NE transect (right-hand side of the island).



### 2.3.5 Aragonite Saturation

The saturation rate of aragonite ( $\Omega_{\text{ar}}$ ) followed the interannual variation of the TA and  $C_T$ .  $\Omega_{\text{ar}}$  were higher than 3 until the top of thermocline, with the highest surface values registered during 2010 cruise (Fig. 12a), and decreased gradually along the depth, varying from 3.92 to 1.02.

**Figure 12:** Vertical distribution of  $\Omega_{ar}$  in 2010 (a), 2012 (b) and 2014 (c) around FNA on the SW transect (left-hand side of the island) and NE transect (right-hand side of the island).



## 2.4 DISCUSSION

The density or thermohaline gradient around FNA showed great stratification, a consequence of annual high insolation and lack of strong upwellings. This thermohaline structure followed the typical vertical distribution for tropical Southwest Atlantic Ocean, represented by a mixed water mass until the base of photic layer (the TSW) and by a deep

pycnocline with high values amplitude in subsurface waters (the SACW) (MEDEIROS et al., 1999; SILVA et al., 2005; STRAMMA et al., 2005).

During the rainy season, the tropical Southwest Atlantic Ocean presents warmer and less salty surface waters in comparison with the dry season (ASSUNÇÃO et al., 2016). This can explain the low surface density registered specially in 2014. Nevertheless, during 2010 cruise it was observed the highest SSS, which increased the density and can be associated with the northernmost ITCZ position ever reached in 30 years for the tropical Atlantic (LEFÈVRE et al., 2013).

This change in the ITCZ position can be related with the El Niño Southern Oscillation (ENSO) happened in the 2009, which diminished the influence of trade winds and the precipitation rate over the tropical Atlantic Ocean (SUTTON et al., 2000; GIANNINI et al., 2001; LEFÈVRE et al., 2013; IBÁNHEZ et al., 2017). In the surround of FNA, the high SSS registered in 2010 resulted in higher surface TA values, in consequence of their strong positive correlations (LEFÈVRE et al., 2010; BONOU et al., 2016). As salinity changed according to the water mass or depth (MILLERO et al., 1998), TA followed its distribution (RIVARO et al., 2010).

The high surface TA values also mean a high buffer capacity to the CO<sub>2</sub> excess from the atmosphere or deep waters (EGLESTON et al., 2010), which is expected for a tropical region (MILLERO et al., 1998; SABINE et al., 2004). Biological activities can influence on buffer capacity, specially at areas where the phytoplankton community present a seasonal significant role in the carbon uptake (LEFÈVRE et al., 2008; MANZELLO et al., 2008). Nevertheless, the linear correlation between TA and salinity suggests that physical processes are the main factors controlling its distribution around FNA (CHOU et al., 2007; GONZÁLES-DÁVILA et al., 2010).

Salinity variation is the main factor considered in most of the TA and C<sub>T</sub> intrinsic relationships in regional or global scale (LEE et al., 2006; LEFÈVRE et al., 2010; RIVARO et al., 2010; BONOU et al., 2016; CARTER et al., 2016; WILLIAMS et al., 2016). Nevertheless, for a vertical distribution it was observed in this study that the use of parameters such as temperature and DO can improve the relationships, specially for C<sub>T</sub> calculation (Fig. 9).

Lefèvre et al. (2010) proposed a regression for TA surface calculation in the western tropical Atlantic, and Lee et al. (2006) proposed for the calculation in a global scale. As TA is a semi-conservative parameter (MILLERO et al., 1998; EGLESTON et al., 2010; MILLERO,

2013), this can explain the not significant differences of the values calculated by using only salinity (LEFÈVRE et al. (2010) and LEE et al. (2006)) and by Eq. (2.1). However, for  $C_T$  calculation the addition of temperature and DO improved significantly the relationships in comparison with the regression proposed by Bonou et al. (2016), due to their indirect correlations with the organic matter remineralization (OMR), carbonate dissolution and biological activity (WHANNINKHOF et al., 1999; JURANEK et al., 2011; WILLIAMS et al., 2016; SAUZEDE et al., 2017).

The OMR process is more evident from the base of photic layer until deep waters due to the lack in primary productivity. Along the depth this process consumes DO and releases nutrients and hydrogen protons ( $H^+$ ) (MELTZER et al., 1997), which reacts with the  $CO_3^{2-}$  decreasing the TA values.  $CO_{2(aq)}$  and  $HCO_3^-$  are also formed by the OMR, explaining the increase in the  $C_T$  values as density increase (CHOU et al., 2007; GONZÁLES-DÁVILA et al., 2010).

At the beginning of pycnocline where there was still light penetration (~1%) and the nutrients concentrations were higher than at the surface due to the OMR process, the [Chl-*a*] reached the DCM (CORDEIRO et al., 2013; SOUZA et al., 2013). During photosynthesis, the phytoplankton uptakes nutrients and  $C_T$ , and releases them during respiration process, which can explain the negative correlations between [Chl-*a*] and DIN/DIP (JIANG & CHAI, 2005).

Due to the deep pycnocline, the distribution of nutrients at the surface was generally scarce and the [Chl-*a*] was around  $0.20 \text{ mg m}^{-3}$ , being considered an oligotrophic region (MELTZER et al., 1997; MEDEIROS et al., 1999; CORDEIRO et al., 2013). Nevertheless, it was observed an increase of surface [Chl-*a*] and nutrients, and a subsurface water rising westward FNA during 2010 and 2014 cruises, which classified the occurrence of the IME process (SOUZA et al., 2013; TCHAMABI et al., 2017).

The IME is related mainly to the currents intensity/direction and island topography (ZHENG & ZHENG, 2004; HASEGAWA et al., 2014; CALDEIRA et al., 2015; GOVE et al., 2015). Strongest periods of the cSEC are between March to July (LUMPKIN & GARZOLI, 2005; TCHAMABI et al., 2017), which included the sampling periods of 2010 and 2014 cruises, and could explain the occurrence of IME. The creation of eddies vortices westward the FNA resulted in a subsurface water rising, which changed the density isoline position and took deeper nutrients-rich waters to the surface, increasing the phytoplankton biomass (CORDEIRO et al., 2013) and the  $C_T$  consume, specially in 2010.

This subsurface water rising and its consequences was similar to what Souza et al. (2013), Andrade et al. (2014); Jales et al. (2015) and Queiroz et al. (2015) found around the seamount and islands, which the [Chl-*a*] increased in a magnitude of  $\sim 1 \text{ mg m}^{-3}$ . Nevertheless, the intensity of the IME around FNA was not strong enough to change significantly the carbon chemistry, by biological carbon uptake or by the influence of deep CO<sub>2</sub>-rich waters.

Aragonite is used by the calcifying organisms to produce or secrete their shells and skeletons (DONEY et al., 2009; XUE et al., 2017), and their saturations states are utilized as reference to the ability of calcium carbonate (CaCO<sub>3</sub>) deposit (SILVERMAN et al., 2007; FEELY et al., 2009). All the water column studied was saturated with these minerals ( $\Omega \geq 1$ ), which is a condition that is more favorable to the calcification process than the dissolution (FEELY et al., 2009).

The saturation state of aragonite, is controlled specially by the salinity due its direct ability to regulate [CaCO<sub>3</sub>] along the water column (XUE et al., 2017), explaining the highest values in 2010 cruise. Since the calcium-to-salinity ratio does not vary more than 1.5% in the ocean, the saturation state is represented essentially by the [CO<sub>3</sub><sup>2-</sup>] (FEELY et al., 2004; XUE et al., 2017). Nevertheless, high values of  $\Omega_{\text{ar}}$  does not necessarily means a rising in the calcification rate by the calcifying organisms (GATTUSO et al., 1998). The increase in temperature can improve the salinity, consequently [CO<sub>3</sub><sup>2-</sup>], but also cause the bleaching process, represented by the death of corals zooxanthellae, and consequently influencing negatively on corals' recruitment and calcification rate (AMARAL et al., 2007; FERREIRA et al., 2012).

## 2.5 CONCLUSIONS

The present study concluded that the occurrence of IME westward FNA can change interannually and is a mechanism that can increase [Chl-*a*] in more than six times. Nevertheless, it was not enough to cause significant changes in the carbon chemistry according to our data, which was more correlated to the thermohaline gradient. This implies that the area around FNA, as located in a tropical region, still have a high buffer capacity to the deep CO<sub>2</sub>-rich waters. The use of temperature and dissolved oxygen can improve regressions for the calculation in a vertical profile of the carbonate system parameters, specially for C<sub>T</sub>.

### 3 CONSIDERAÇÕES FINAIS

O presente trabalho conseguiu cumprir com o seu principal objetivo de caracterizar os parâmetros do sistema carbonato na área em torno do Arquipélago de Fernando de Noronha. Esses parâmetros seguiram a distribuição termohalina, o esperado para uma região tropical. A estrutura termohalina ou de densidade mostrou uma forte estratificação vertical, típica de uma região tropical, responsável por limitar maiores concentrações de nutrientes dissolvidos na superfície. No entanto, durante as campanhas realizadas no mês de julho (2010, 2014) foi registrado uma pequena ascendência da picnoclina a jusante da ilha, o que possibilitou o aumento da concentração superficial de clorofila-*a* e dos nutrientes inorgânicos dissolvidos avaliados.

O aumento de clorofila-*a* (em mais de 6 vezes) e dos nutrientes inorgânicos dissolvidos superficiais no lado oeste da ilha confirma a ocorrência do Efeito Ilha, e os períodos estudados mostram que há uma variação interanual, que de acordo com nossas análises foi significativa para clorofila-*a*. Isso se deve, segundo a bibliografia estudada, à variabilidade espaço-temporal do ramo central da Corrente Sul Equatorial. Para corroborar com os dados obtidos no presente estudo se faz necessária uma maior periodicidade de campanhas oceanográficas na área em torno de Fernando de Noronha, para avaliar com mais detalhes a variabilidade espaço temporal desses parâmetros.

Em um perfil vertical, a inclusão de parâmetros como temperatura e oxigênio dissolvido se mostrou mais eficiente para o cálculo dos parâmetros do sistema carbonato, principalmente do carbono inorgânico dissolvido total, garantindo indiretamente a influência de processos como a remineralização da matéria orgânica e dissolução de carbonatos. Variações na distribuição dos parâmetros do sistema carbonato entre os períodos estudados e entre os lados da ilha não foram observadas, o que leva a concluir que o sistema carbonato não foi significativamente influenciado pelo Efeito Ilha.

## REFERÊNCIAS

- ALMEIDA, F. F. M. Ilhas oceânicas brasileiras e suas relações com a tectônica atlântica. **Terrae Didatica** v. 2, n. 1, p. 3-18, 2006.
- AMARAL, F. D.; HUDSON, M. M.; STEINER, A. Q.; RAMOS, C. A. C. Corals and calcified hydroids of the Manuel Luiz Marine State Park (State of Maranhão, Northeast Brazil). **Biota Neotropica**, v. 7, n. 3 p. 73-81, 2007.
- ANDRADE, I.; SANGRÀ, P.; HORMAZABAL, S.; CORREA-RAMIREZ, M. Island mass effect in the Juan Fernández Archipelago (33 S), southeastern Pacific. **Deep Sea Research Part I: Oceanographic Research Papers**, v. 84, p. 86-99, 2014.
- ASSUNÇÃO, R. V.; SILVA, A. C.; MARTINS, J.; FLORES-MONTES, M. Spatial-Temporal Variability of the Thermohaline Properties in the Coastal Region of Fernando de Noronha Archipelago, Brazil. **Journal of Coastal Research**, v. 75, n. sp1, p. 512-516, 2016.
- BARCELLOS, R. L.; LINS, S. R.; COELHO-JR, C.; TRAVASSOS, P. E. Processos sedimentares sazonais e análise da fração arenosa no sistema ambiental do sueste, Fernando de Noronha, estado de Pernambuco. **Arquivos de Ciências do Mar**, v. 50, n. 1, p. 42-71, 2017.
- BARTON, E. D. Island wakes. **Encyclopedia of ocean sciences**, v. 3, p. 1397-1403, 2001.
- BASTERRETSEA, G.; BARTONB, E. D.; TETTC, P.; SANGRÁ, P.; NAVARRO-PEREZB, E.; ARÍSTEGUID, J. Eddy and deep chlorophyl maximum response to wind-shear in the lee of Gran Canaria. **Deep Sea Research Part I: Oceanographic Research Papers**, v. 49, n. 6, p. 1087-1101, 2002.
- BONOU, F. K. Variabilidade dos parâmetros de controle do CO<sub>2</sub> na borda oeste do Atlântico tropical. **Tese de Doutorado Universidade Federal de Pernambuco**, 2016.
- BONOU, F. K.; NORIEGA, C.; LEFÈVRE, N.; ARAUJO, M. Distribution of CO<sub>2</sub> parameters in the Western Tropical Atlantic Ocean. **Dynamics of Atmospheres and Oceans**, v. 73, p. 47-60, 2016.
- CALDEIRA, R. M. A.; MARCHESIELLO, P. Ocean response to wind sheltering in the Southern California Bight. **Geophysical research letters**, v. 29, n. 3, 2002.
- CALDEIRA, R. M. A.; GROOM, S.; MILLER, P.; PILGRIM, D.; NEZLIN, N. P. Sea-surface signatures of the island mass effect phenomena around Madeira Island, Northeast Atlantic. **Remote Sensing of Environment**, v. 80, p. 336-360, 2002.

- CALDEIRA, R. M.; MARCHESIELLO, P.; NEZLIN, N. P.; DIGIACOMO, P. M.; MCWILLIAMS, J. C. Island wakes in the southern California Bight. **Journal of Geophysical Research: Oceans**, v. 110, n. C11, 2005.
- CARTER, B. R.; WILLIAMS, N. L.; GRAY, A. R.; FEELY, R. A. Locally interpolated alkalinity regression for global alkalinity estimation. **Limnology and Oceanography: Methods**, v. 14, n. 4, p. 268-277, 2016.
- CHANG, M. H.; TANG, T. Y.; HO, C. R.; CHAO, S. Y. Kuroshio-induced wake in the lee of Green Island off Taiwan. **Journal of Geophysical Research: Oceans**, v. 118, n. 3, 1508-1519, 2013.
- CHOU, W. C.; SHEU, D. D.; LEE, B. S.; TSENG, C. M.; CHEN, C. T. A.; WANG, S. L.; WONG, G. T. F. Depth distributions of alkalinity, TCO<sub>2</sub> and δ<sup>13</sup>CTCO<sub>2</sub> at SEATS time-series site in the northern South China Sea. **Deep Sea Research Part II: Topical Studies in Oceanography**, v. 54, n. 4, p. 1469-1485, 2007.
- CORDEIRO, T. A.; BRANDINI, F. P.; ROSA, R. S.; SASSI, R. Deep Chlorophyll Maximum in Western Equatorial Atlantic-How does it Interact with Islands Slopes and Seamounts? **Marine Science**, v. 3, n. 1, p. 30-37, 2013.
- COUTIS, P. F.; MIDDLETON, J. H. The physical and biological impact of a small island wake in the deep ocean. **Deep Sea Research Part I: Oceanographic Research Papers**, v. 49, n. 8, p. 1341-1361, 2002.
- DICKSON, A. G.; GOYET, C. Handbook of methods for the analysis of the various parameters of the carbon dioxide system in sea water. **ORNL/CDIAC-74**, v. 107, 1994.
- DICKSON, A. G.; MILLERO, F. J. A comparison of the equilibrium constants for the dissociation of carbonic acid in seawater media. **Deep Sea Research Part A. Oceanographic Research Papers**, v. 34, n. 10, p. 1733-1743, 1987.
- DICKSON, A. G.; SABINE, C. L.; CHRISTIAN, J. R. Guide to best practices for ocean CO<sub>2</sub> measurements. **PICES Special Publication**, v. 3, p. 191, 2007.
- DONEY, S. C.; MAHOWALD, N.; LIMA, I.; FEELY, R. A.; MACKENZIE, F. T.; LAMARQUE, J-F.; RASCH, P. J. Impact of anthropogenic atmospheric nitrogen and sulfur deposition on ocean acidification and the inorganic carbon system. **Proceedings of the National Academy of Sciences**, v. 104, n. 37, p. 14580-14585, 2007.

- DONEY, S. C.; FABRY, V. J.; FEELY, R. A.; KLEYPAS, J. A. Ocean acidification: the other CO<sub>2</sub> problem. **Annual Review of Marine Science**, v. 1, p. 169-192, 2009.
- DOTY, M. S.; OGURI, M. The island mass effect. **ICES Journal of Marine Science**, v. 22, n. 1, p. 33-37, 1956.
- EDMOND, J. M. High precision determination of titration alkalinity and total carbon dioxide content of seawater by potentiometric titration. **Deep Sea Research**, v. 17, n. 4, p. 737-750, 1970.
- EGLESTON, E. S.; SABINE, C. L.; MOREL, F. M. Revelle revisited: Buffer factors that quantify the response of ocean chemistry to changes in DIC and alkalinity. **Global Biogeochemical Cycles**, v. 24, n. 1, 2010.
- FEELY, R. A.; DONEY, S. C.; COOLEY, S. R. Ocean acidification: Present conditions and future changes in a high-CO<sub>2</sub> world. **Oceanography**, v. 22, n. 4, p. 36-47, 2009.
- FEELY, R. A.; SABINE, C. L.; LEE, K.; BERELSON, W.; KLEYPAS, J.; FABRY, V. J.; MILLERO, F. J. Impact of anthropogenic CO<sub>2</sub> on the CaCO<sub>3</sub> system in the oceans. **Science**, v. 305, n. 5682, p. 362-366, 2004.
- FLORES MONTES, M. J. Fatores que influenciam na produtividade dos oceanos: a importância do fluxo de difusão dos nutrientes para a biomassa do fitoplâncton na região oceânica do nordeste brasileiro. **Tese de Doutorado Universidade Federal de Pernambuco**, 2003.
- FERREIRA, B. P.; COSTA, M. B. S. F.; COXEY, M. S.; GASPAR, A. L. B.; VELEDA, D.; ARAUJO, M. The effects of sea surface temperature anomalies on oceanic coral reef systems in the southwestern tropical Atlantic. **Coral reefs**, v. 32, n. 2, p. 441-454, 2013.
- GATTUSO, J. P.; FRANKIGNOULLE, M.; BOURGE, I.; ROMAINE, S.; BUDDEMEIER, R. W. Effect of calcium carbonate saturation of seawater on coral calcification. **Global and Planetary Change**, v. 18, n. 1, p. 37-46, 1998.
- GIANNINI, A.; CHIANG, J. C.; CANE, M. A.; KUSHNIR, Y.; SEAGER, R. The ENSO teleconnection to the tropical Atlantic Ocean: Contributions of the remote and local SSTs to rainfall variability in the tropical Americas. **Journal of Climate**, v. 14, n. 24, p. 4530-4544, 2001.

- GONZÁLES-DÁVILA, M.; SANTANA-CASIANO, J. M.; RUEDA, M. J.; LLINÁS, O. The water column distribution of carbonate system variables at the ESTOC site from 1995 to 2004. **Biogeosciences**, v. 7, n. 10, p. 3067, 2010.
- GOVE, J. M. Upwelling variability at Jarvis Island. **Tese de Doutorado University of Hawaii at Manoa**, 2005.
- GOVE, J. M.; MERRIFIELD, M. A.; BRAINARD, R. E. Temporal variability of current-driven upwelling at Jarvis Island. **Journal of Geophysical Research: Oceans**, v. 111, n. C12, 2006.
- GOVE, J. M.; MCMANUS, M. A.; NEUHEIMER, A. B.; POLOVINA, J. J.; DRAZEN, J. C.; SMITH, C. R.; MERRIFIELD, M. A.; FRIEDLANDER, A. M.; EHSES, J. S.; YOUNG, C. W.; DILLON, A. K.; WILLIAMS, G. J. Near-island biological hotspots in barren ocean basins. **Nature communications**, v. 7, p. 10581, 2016.
- GRASSHOFF, K.; KREMLING, K.; EHRHARD, M. Methods of Seawater Analysis. **Verlag Chemie**, v. 317, 1993.
- HARLAN, J. A.; SWEARER, S. E.; LEBEN, R. R.; FOX, C. A. Surface circulation in a Caribbean island wake. **Continental Shelf Research**, v. 22, n. 3, p. 417-434, 2002.
- HASEGAWA, D.; YAMAZAKI, H.; LUECK, R. G.; SEURONT, L. How islands stir and fertilize the upper ocean. **Geophysical research letters**, v. 31, n. 16, 2004.
- HEYWOOD, K. J.; BARTON, E. D.; SIMPSON, J. H. The effects of flow disturbance by an oceanic island. **Journal of Marine Research**, v. 48, n. 1, p. 55-73, 1990.
- HEYWOOD, K. J.; STEVENS, D. P.; BIGG, G. R. Eddy formation behind the tropical island of Aldabra. **Deep Sea Research Part I: Oceanographic Research Papers**, v. 43, n. 4, p. 555-578, 1996.
- HAZIN, F. H. V.; ZAGAGLIA, J. R.; BROADHURST, M. K.; TRAVASSOS, P. E. P.; BEZERRA, T. R. Q. Review of a small-scale pelagic longline fishery off northeastern Brazil. **Marine Fisheries Review**, v. 60, n. 3, p. 1-8, 1998.
- IBÁÑEZ, J. S. P.; FLORES-MONTES, M.; LEFÈVRE, N. Collapse of the tropical and subtropical North Atlantic CO<sub>2</sub> sink in boreal spring of 2010. **Scientific Reports**, v. 7, 2017.
- JALES, M. C.; FEITOSA, F. A. D. N.; KOENING, M. L.; FLORES-MONTES, M.; ARAÚJO FILHO, M. C. D.; SILVA, R. A. D. Phytoplankton biomass dynamics and environmental

variables around the Rocas Atoll Biological Reserve, South Atlantic. **Brazilian Journal of Oceanography**, v. 63, n. 4, p. 443-454, 2015.

JIANG, M. S.; CHAI, F. Physical and biological controls on the latitudinal asymmetry of surface nutrients and pCO<sub>2</sub> in the central and eastern equatorial Pacific. **Journal of Geophysical Research: Oceans**, v. 110, n. C16, 2005.

JURANEK, L. W.; FEELY, R. A.; GILBERT, D.; FREELAND, H.; MILLER, L. A. Real-time estimation of pH and aragonite saturation state from Argo profiling floats: Prospects for an autonomous carbon observing strategy. **Geophysical Research Letters**, v. 38, n. 17, 2011.

KITIDIS, V.; BROWN, I.; HARDMA-MOUNTFORD, N.; LEFÈVRE, N. Surface ocean carbon dioxide during the Atlantic Meridional Transect (1995–2013); evidence of ocean acidification. **Progress in Oceanography**, 2016.

LEE, K.; TONG, L. T.; MILLERO, F. J.; SABINE, C. L.; DICKSON, A. G.; GOYET, C.; PARK, G-H.; WANNINKHOF, R.; FEELY, R. A; KEY, R. M. Global relationships of total alkalinity with salinity and temperature in surface waters of the world's oceans. **Geophysical Research Letters**, v. 33, n. 19, 2006.

LEFÈVRE, N.; GUILLOT, A.; BEAUMONT, L.; DANGUY, T. Variability of fCO<sub>2</sub> in the Eastern Tropical Atlantic from a moored buoy. **Journal of Geophysical Research: Oceans**, v. 113, n. C1, 2008.

LEFÈVRE, N.; DIVERRÈS, D.; GALLOIS, F. Origin of CO<sub>2</sub> undersaturation in the western tropical Atlantic. **Tellus B**, v. 62, n. 5, p. 595-607, 2010.

LEFÈVRE, N.; CANIAUX, G.; JANICOT, S.; GUEYE, A. K. Increased CO<sub>2</sub> outgassing in February-May 2010 in the tropical Atlantic following the 2009 Pacific El Niño. **Journal of Geophysical Research: Oceans**, v. 118, n. 4, p. 1645-1657, 2013.

LEFÈVRE, N., FLORES-MONTES, M.; GASPAR, F. L.; ROCHA, C.; JIANG, S.; ARAÚJO, M. C.; IBÁNHEZ, J. Net Heterotrophy in the Amazon Continental Shelf Changes Rapidly to a Sink of CO<sub>2</sub> in the Outer Amazon Plume. **Frontiers in Marine Science**, v. 4, p. 278, 2017.

LIMA, A. R.; BARLLETA, M.; COSTA, M. F. Seasonal-dial shifts of ichthyoplankton assemblages and plastic debris around an Equatorial Atlantic archipelago. **Frontiers in Environmental Science**, v. 4, p. 56, 2016.

- LIRA, S. M. D. A.; TEIXEIRA, I. D. Á.; LIMA, C. D. M. D.; SANTOS, G. D. S.; LEITÃO, S. N.; SCHWAMBORN, R. Spatial and nycthemeral distribution of the zooneuston off Fernando de Noronha, Brazil. **Brazilian Journal of Oceanography**, v. 62, n. 1, p. 35-45, 2014.
- LUMPKIN, R.; GARZOLI, S. L. Near-surface circulation in the tropical Atlantic Ocean. **Deep Sea Research Part I: Oceanographic Research Papers**, v. 52, n. 3, p. 495-518, 2005.
- MACEDO, S. J.; FLORES-MONTES, M. J.; LINS, I. C.; COSTA, K. M. P. REVIZEE – Programa da avaliação do Potencial Sustentável dos Recursos Vivos da Zona Econômica Exclusiva. SCORE/NE. In: **Relatório da Oceanografia Química Universidade Federal de Pernambuco**, 1998.
- MANZELLO, D. P.; KLEYPAS, J. A.; BUDD, D. A.; EAKIN, C. M.; GLYNN, P. W.; LANGDON, C. Poorly cemented coral reefs of the eastern tropical Pacific: Possible insights into reef development in a high-CO<sub>2</sub> world. **Proceedings of the National Academy of Sciences**, v. 105, n. 30, p. 10450-10455, 2008.
- MARQUES, F. A.; ROSAS, M. R.; BRETAS, S. M. B.; NOVAIS, A. T. F., WANDERLEY, J. F. F. L. Caracterização e classificação de Neossolos da ilha de Fernando de Noronha (PE). **Revista Brasileira de Ciência do Solo**, v. 31, n. 6, 2007.
- MEDEIROS, C.; MACEDO, S. J.; FEITOSA, F. A. N.; KOENING, M. L. Hydrography and phytoplankton biomass and abundance of north-east Brazilian Waters. **Archiv fuer Fischerei und Meeresforschung**, v. 47, p. 133–151, 1999.
- MEHRBACH, C.; CULBERSON, C. H.; HAWLEY, J. E; PYTKOWICZ, R. M. Measurement of the Apparent Dissociation Constants of Carbonic Acid in Seawater at Atmospheric Pressure. **Limnology and Oceanography**, v. 18, n. 6, p. 897-907, 1973.
- METZLER, P. M.; GLIBERT, P. M.; GAETA, S. A.; LUDLAM, J. M. New and regenerated production in the South Atlantic off Brazil. **Deep Sea Research Part I: Oceanographic Research Papers**, v. 44, n. 3, p. 363-384, 1997.
- MILLERO, F. J.; LEE, K.; ROCHE, M. Distribution of alkalinity in the surface waters of the major oceans. **Marine Chemistry**, v. 60, n. 1, p. 111-130, 1998.
- MILLERO, F. J. Chemical oceanography, **CRC press**, 2013.
- MOLINARI, R. L. Observations of eastward currents in the tropical South Atlantic Ocean: 1978–1980. **Journal of Geophysical Research: Oceans**, v. 87, n. C12, p. 9707-9714, 1982.

NORZAGARAY-LÓPEZ, C. O.; HERNÁNDEZ-AYÓN, J. M.; CALDERON AGUILERA, L. E.; REYES-BONILLA, H.; CHAPA-BALCORTA, C.; AYALA-BOCOS, A. Aragonite saturation and pH variation in a fringing reef are strongly influenced by oceanic conditions. **Limnology and Oceanography**, v. 62, n. 6, p. 2375-2388, 2017.

OLSEN, A.; KEY, R. M.; HEUVEN, S. V.; LAUVSET, S. K.; VELO, A.; LIN, X.; SCHIRNICK, C.; KOZYR, A.; TANHUA, T.; HOPPEMA, M.; JUTTERSTROM, S.; STEINFELDT, R.; JEANSSON, E.; ISHII, M.; PÉREZ, F. F.; SUZUKI, T. The Global Ocean Data Analysis Project version 2 (GLODAPv2)—an internally consistent data product for the world ocean. **Earth System Science Data**, v. 8, n. 2, p. 297, 2016.

PINHEIRO, H. T.; BERNADI, G.; SIMON, T.; JOYEUX, J-C.; MACIEIRA, R. M.; GASPARINI, J. L.; ROCHA, C.; ROCHA, L. A. Island biogeography of marine organisms. **Nature**, v. 549, n. 7670, p. 82, 2017.

PIONTKOVSKI, S. A.; LANDRY, M. R.; FINENKO, Z. Z.; KOVALEY, A. V.; WILLIAMS, R.; GALLIENNE, C. P.; MISHONOV, A. V.; SKRYABIN, V. A.; TOKAREY, Y. N.; NIKOLSKY, V. N. Plankton communities of the South Atlantic anticyclonic gyre. **Oceanologica Acta**, v. 26, n. 3, p. 255-268, 2003.

QUEIROZ, A. R.; FLORES-MONTES, M.; CASTRO P. A. M. M.; SILVA, R. A.; KOENING, M. L. Vertical and horizontal distribution of phytoplankton around an oceanic archipelago of the Equatorial Atlantic. **Marine Biodiversity Records**, v. 8, 2015.

REVERDIN, G.; RUAL, P.; PENHOAT, Y. D.; GOURIOU, Y. Vertical structure of the seasonal cycle in the central equatorial Atlantic Ocean: XBT sections from 1980 to 1988. **Journal of Physical Oceanography**, v. 21, n. 2, p. 277-291, 1991.

RIVARO, P.; MESSA, R.; MASSOLO, S.; FRACHE, R. Distributions of carbonate properties along the water column in the Mediterranean Sea: Spatial and temporal variations. **Marine Chemistry**, v. 121, n. 1, p. 236-245, 2010.

SABINE, C. L.; FEELY, R. A.; GRUBER, N.; KEY, R. M.; LEE, K.; BULLISTER, J. L.; WANNINKHOF, R.; WONG, C. S.; WALLACE, D. W. R.; TILBROOD, B.; MILLERO, F. J.; PENG, T-H.; KOZYR, A.; ONO, T.; RIOS, A. F. The oceanic sink for anthropogenic CO<sub>2</sub>. **Science**, v. 305, n. 5682, p. 367-371, 2004.

SAMPAIO, C. L.; NUNES, J. D. A. C.; MENDES, L. F. *Acyrtus pauciradiatus*, a new species of clingfish (Teleostei: Gobiesocidae) from Fernando de Noronha Archipelago, Pernambuco state, Northeastern Brazil. **Neotropical Ichthyology**, v. 2, n. 4, p. 206-208, 2004.

SAUZÈDE, R.; BITTIG, H. C.; CLAUSTRE, H.; FOMMERVAULT, O. P.; GATTUSO, J. P.; LEGENDRE, L.; JOHNSON, K. S. Estimates of Water-Column Nutrient Concentrations and Carbonate System Parameters in the Global Ocean: A Novel Approach Based on Neural Networks. **Frontiers in Marine Science**, vol. 4, 2017.

SERAFINI, T. Z.; FRANÇA, G. B.; ANDRIGUETTO-FILHO, J. M. Ilhas oceânicas brasileiras: biodiversidade conhecida e sua relação com o histórico de uso e ocupação humana. **Revista de Gestão Costeira Integrada**, v. 10, n. 3, 2010.

SCHOTT, F. A.; DENGLER, M.; BRANDT, P.; AFFLER, K.; FISCHER, J.; BOURLES, B.; YVES, G.; ROBERT, L. MOLINARI; RHEIN, M. The zonal currents and transports at 35 W in the tropical Atlantic. **Geophysical Research Letters**, vol. 30, n. 7, 2003.

SILVA, A. C. D.; ARAÚJO, M.; BOURLÈS, B. Variação sazonal da estrutura de massas de água na plataforma continental do Amazonas e área oceânica adjacente. **Revista Brasileira de Geofísica**, vol. 23, n. 2, p. 145-157, 2005.

SILVA, M. A.; Caracterização da estrutura termohalina no etorno das ilhas oceânicas de Fernando de Noronhas, Atol das Rocas e São Pedro e São Paulo. **Monografia Universidade Federal de Pernambuco**, 2016.

SILVERMAN, J.; LAZAR, B.; EREAZ, J. Effect of aragonite saturation, temperature, and nutrients on the community calcification rate of a coral reef. **Journal of Geophysical Research: Oceans**, vol. 112, n. C5, 2007.

SOUZA, C. S.; LUZ, J. A. G.; MACEDO, S.; FLORES-MONTES, M.; MAFALDA, P. Chlorophyll a and nutrient distribution around seamounts and islands of the tropical southwestern Atlantic. **Marine and Freshwater Research**, vol. 64, n. 2, p. 168-184, 2013.

STRAMMA, L.; ENGLAND, M. On the water masses and mean circulation of the South Atlantic Ocean. **Journal of Geophysical Research: Oceans**, vol. 104, n. C9, p. 20863-20883, 1999.

STRAMMA, L.; SCHOTT, F. The mean flow field of the tropical Atlantic Ocean. **Deep Sea Research Part II: Topical Studies in Oceanography**, vol. 46, n. 1, p. 279-303, 1999.

- STRAMMA, L.; RHEIN, M.; BRANDT, P.; DENGLER, M.; BONING, C.; WALTER, M. Upper ocean circulation in the western tropical Atlantic in boreal fall 2000. **Deep Sea Research Part I: Oceanographic Research Papers**, vol. 52, n. 2, p. 221-240, 2005.
- STRICKLAND, J. D.; PARSONS, T. R. A practical handbook of seawater analysis, 1972.
- SUTTON, R. T.; JEWSON, S. P.; ROWELL, D. P. The elements of climate variability in the tropical Atlantic region. **Journal of Climate**, vol. 13, n. 18, p. 3261-3284, 2000.
- TAKAHASHI, T.; SUTHERLAND, S. C.; WANNINKHOF, R.; SWEENEY, C.; FEELY, R. A.; CHIPMAN, D. W.; HALES, B.; FRIEDERICH, G.; CHAVEZ, F.; SABINE, C.; WATSON, A.; BAKKER, D. C. E.; SCHUSTER, U.; METZL, N.; YOSHIKAWA-INOUE, H.; ISHII, M.; MIDORIKAWA, T.; NOJIRI, Y.; KORTZINGER, A.; STEINHOFF, T.; HOPPEMA, M.; OLAFSSON, J.; ARNARSON, T.; TILBROOK, B.; JOHANNESSEN, T.; OLSEN, A.; BELLERBY, R.; WONG, C. S.; DELILLE, B.; BATES, N. R.; BAAR, H. J. W. Climatological mean and decadal change in surface ocean pCO<sub>2</sub>, and net sea-air CO<sub>2</sub> flux over the global oceans. **Deep Sea Research Part II: Topical Studies in Oceanography**, v. 56, n. 8, p. 554-577, 2009.
- TCHAMABI, C. C.; ARAÚJO, M.; SILVA, M.; BOURLÈS, B. A study of the Brazilian Fernando de Noronha island and Rocas atoll wakes in the tropical Atlantic. **Ocean Modelling**, vol. 111, p. 9-18, 2017.
- TEAGUE, W. J.; HWANG, P. A.; JACOBS, G. A.; BOOK, J. W.; PERKINS, H. T. Transport variability across the Korea/Tsushima Strait and the Tsushima Island wake. **Deep Sea Research Part II: Topical Studies in Oceanography**, v. 52, n. 11-13, p. 1784-1801, 2005.
- WANNINKHOF, R.; DONEY, S. C.; PENG, T. H.; BULLISTER, J. L.; LEE, K.; FEELY, R. A. Comparison of methods to determine the anthropogenic CO<sub>2</sub> invasion into the Atlantic Ocean. **Tellus B: Chemical and Physical Meteorology**, vol. 51, n. 2, p. 511-530, 1999.
- WILLIAMS, N. L.; JURANEK, L. W.; JOHNSON, K. S.; FEELY, R. A.; RISER, S. C.; TALLEY, L. D.; RUSSEL, J. L.; SARMIENTO, J. L.; WANNINKHOF, R. Empirical algorithms to estimate water column pH in the Southern Ocean. **Geophysical Research Letters**, vol. 43, n. 7, p. 3415-3422, 2016.
- XUE, L.; CAI, W. J.; SUTTON, A. J.; SABINE, C. Sea surface aragonite saturation state variations and control mechanisms at the Gray's Reef time-series site off Georgia, USA (2006–2007). **Marine Chemistry**, 2017

ZHENG, Z. W.; ZHENG, Q. Variability of island-induced ocean vortex trains, in the Kuroshio region southeast of Taiwan Island. **Continental Shelf Research**, vol. 81, p. 1-6, 2014.

## APÊNDICE

**Figure S1:** Mean halocline in 2010 (a), 2012 (b) and 2014 (c) upstream (right-hand side) and downstream (left-hand side) FNA.

